Using Mussel Transcriptomics for Environmental Monitoring in Port Valdez, Alaska: 2019 and 2020 Pilot Study Results

PWSRCAC Contract number: 951.21.06

February 17, 2021

Lizabeth Bowen[1], Austin Love[2], Shannon Waters[1], Katrina Counihan[3], Brenda Ballachey[4], Heather Coletti[5], William B. Driskell[6], and James R. Payne[7]

[1]U.S. Geological Survey, Western Ecological Research Center, Davis, CA 95616 USA.

lbowen@ucdavis.edu. 530-752-5365

[2]Prince William Sound Regional Citizens' Advisory Council, Valdez, AK, USA.

[3]Alaska SeaLife Center, Seward, AK 99664 USA

[4]U.S. Geological Survey (Emeritus), Alaska Science Center, Anchorage, AK, USA

[5]National Park Service, Inventory & Monitoring Program, Southwest Alaska Network, Anchorage, AK, USA

[6]Independent Consultant, Seattle, WA, USA

[7]Payne Environmental Consultants, Inc., Encinitas, CA, USA

TABLE OF CONTENTS

ACRONYMS

AMT – Saw Island sample site

ANS – Alaska North Slope

B[a]P – benzo[a]pyrene

CaM – Calmodulin gene

Casp8 – Caspase 8 gene

CCOIV – Cytochrome C Oxidase IV gene

cDNA – complementary deoxyribonucleic acid

CHI – Chitinase gene

CNN – Calponin gene

Cyp3 – Cytochrome P450 family 3 gene

C_T – cycle threshold crossing values

GB – Galena Bay sample site

GoC – Gold Creek sample site

Harbor – Whittier Harbor, Seward Harbor and Cordova Harbor sample sites

HIFa – hypoxia-inducible factor alpha gene

HSP70 – heat shock protein 70 gene

HSP90 – heat shock protein 90 gene

JPO – Jackson Point sample site

JB – Jack Bay sample site

KATM – Katmai National Park

LACL – Lake Clark National Park

LTEMP – Long-Term Environmental Monitoring Program

mRNA – messenger ribonucleic acid

MIF – macrophage migration inhibitory factor gene

MT20 – Metallothionein 20 gene

Myt – Mytilin gene

MytB – Myticin B gene

NMDS – non-parametric multidimensional scaling

NPP- National Park and Preserve

PAH – polycyclic aromatic hydrocarbons

PCR – polymerase chain reaction

PWS – Prince William Sound

PWS Field – Herring Bay, Hogan Bay, Iktua Bay, Johnson Bay, and Whale Bay sample sites

PWSRCAC – Prince William Sound Regional Citizens' Advisory Council

P53 – tumor protein 53 gene

RNA – ribonucleic acid
SAC – Scientific Advisory Committee
USGS – United States Geological Survey
VH – Valdez Small Boat Harbor sample site
18S – ribosomal reference gene

INTRODUCTION

This project was inspired by a Prince William Sound Regional Citizens' Advisory Council (PWSRCAC) 2018 Science Night presentation of work by Dr. Katrina Counihan from the Alaska SeaLife Center. The results comprised mussel and razor clam genetic transcription experiments she conducted in Southcentral Alaska. Through Dr. Counihan's work, the Council was introduced to another researcher, Dr. Lizabeth Bowen, an ecologist with the United States Geological Survey (USGS), who was the lead author of a 2018 research paper titled "Gene transcription patterns in response to low level petroleum contaminants in Mytilus trossulus [Bay mussels] from field sites and harbors in southcentral Alaska," in Deep-Sea Research Part II.

Dr. Bowen's 2018 paper looked at whether mussel gene transcription is affected by oil pollution and other environmental factors. Dr. Bowen's research included five locations in Prince William Sound (PWS), Alaska, that were oiled during the Exxon Valdez oil spill and three harbors in the Exxon Valdez oil spill region: Seward, Whittier, and Cordova.

Exposure to contaminants, including polycyclic aromatic hydrocarbons (PAHs) found in crude oil, can lead to pathophysiological changes that may be subtle but significant, and difficult to detect using classical biological or chemical diagnostic methods. The earliest observable indications of physiological impairment can be altered levels of gene transcripts, evident prior to clinical signs (Farr and Dunn, 1999; McLoughlin et al., 2006; Poynton and Vulpe, 2009). Gene transcription is the process by which information from the DNA template of a particular gene is transcribed into messenger ribonucleic acid (mRNA) and eventually translated into a functional protein. Quantitative analysis of mRNA therefore is used as a measure of gene transcription (Heid et al., 1996). The amount of a particular gene that is transcribed is physiologically dictated by a number of intrinsic and extrinsic factors, including stimuli such as infectious agents, toxin exposure, trauma, or neoplasia. For the interests of this study, gene transcription assays measure the

physiological response of an organism to xenobiotic oil contaminants. Furthermore, the deleterious effects of toxic exposure may persist beyond metabolism and excretion of the toxin. Gene expression assays are advantaged by the ability to measure the persistent physiologic responses of an individual to the metabolic stimuli, independent of the continued presence of the original toxin or its metabolites.

This two-year project is a pilot study designed to mirror previous mussel transcriptomic research conducted by Dr. Bowen and Dr. Counihan in Southcentral Alaska. The goal is to determine if transcriptomic analysis of mussel tissue would be useful as a part of the Council's Long-Term Environmental Monitoring Program (LTEMP).

METHODS

Mussel collection and tissue preservation

Mussels were collected in June 2019 and 2020, from each of four locations in Port Valdez: Saw Island (AMT), Jackson Point (JPO), Gold Creek (GoC), and the Valdez Small Boat Harbor (VH) (**Figure 1**). AMT, JPO, and GoC are "traditional" LTEMP sites. VH, a location of known mixed petroleum and pyrogenic contamination, was sampled as a strong "positive control" site to better understand how transcription reacts to chronic levels of petroleum contamination. In 2019, the VH mussels were collected from a creosote piling. We note that creosote leachates are not the same weathered Alaska North Slope (ANS) crude oil being released at the terminal albeit similar constituents are present. In 2020, the VH mussels were collected from boulder riprap exposed to vessel traffic in the harbor entrance where, although still not weathered ANS crude oil, there are sources of ANS derived fuel and oils in the chemical profiles.

In contrast to VH, GoC is relatively far from known sources of hydrocarbon contamination; therefore, it was chosen as the clean control site to compare to other sampling locations. However, the June 2019 transcriptomics results indicated that GoC may not be as free from petroleum contamination as hoped. In June 2020, two additional sites (Jack Bay (JB) and Galena Bay (GB)) more remote in Valdez Arm were sampled as alternative clean control sites (**Figure 2**).

The GB location was an intertidal site previously sampled through the Gulf Watch Alaska's environmental monitoring program – but is currently not actively sampled in that program. The JB site is not known to have been previously sampled by the Gulf Watch or other environmental monitoring programs but was selected due to its distance from known sources of petroleum contamination.

Procedurally, after the mussels were collected their gill and adductor muscle tissues were extracted, preserved in RNAlater, and frozen for further analysis. At each sampling location

mussels were sampled from various heights of the intertidal zone. Three replicate samples of 10 mussels were collected from each location. The 10 mussels for each replicate were generally collected along a 2 meter section of shoreline. Relatively larger mussels were sampled for ease of dissecting gill and adductor tissues, and no morphometric data was collected.

On April 12, 2020, there was an oil spill from the Valdez Marine Terminal. Additional mussels were collected from April through August 2020, for transcriptomic and chemical analysis. The results of those analyses associated with the mussels collected in response to the April 12 oil spill will be described in a separate report and manuscript.

Figure 1. Map of Port Valdez showing the four mussel transcriptomics locations sampled in 2019 & 2020 (Source: Google Earth).

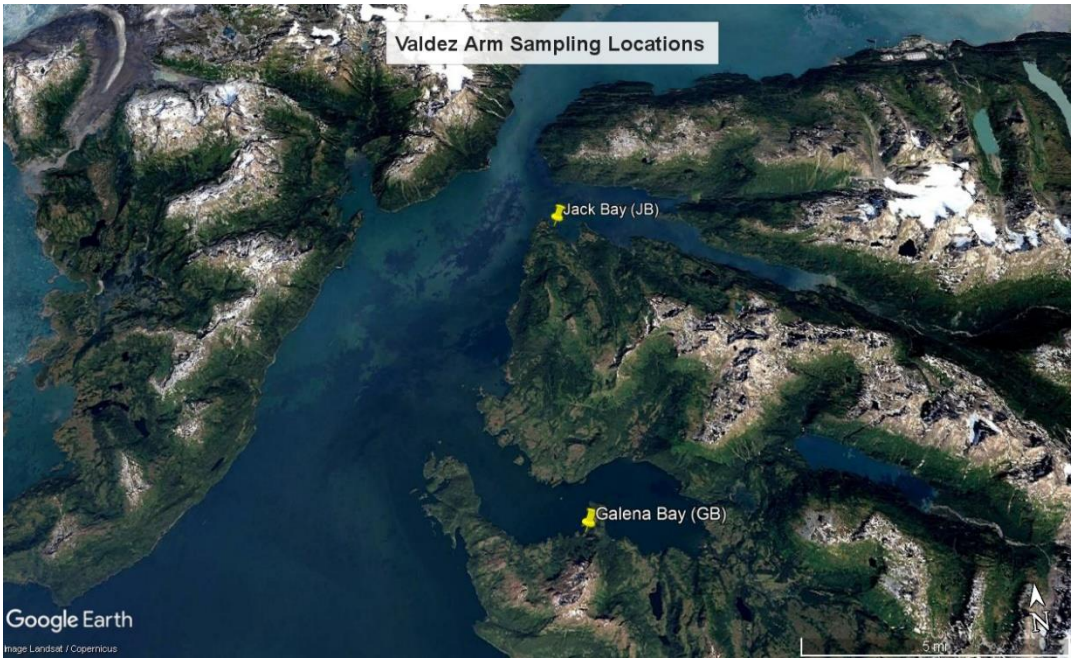

Figure 2. Map of the Valdez Arm showing the two mussel transcriptomics locations sampled in 2020 (Source: Google Earth).

Previously Available Samples

Although this study was focused on sites in Port Valdez and the Valdez Arm (LTEMP sites), we had the opportunity to compare these samples with previously published data (Bowen et al. 2018, Counihan et al. 2019). These data include mussel samples from Katmai (KATM) and Lake Clark National Parks (LACL) in 2015-2016 (**Figure 3**), as well as various locations in and around PWS in 2012-2015 (**Figure 4**). The 2012-2015 PWS samples include mussels taken from three harbor locations (Whittier, Seward, and Cordova Harbor) and five field locations (Herring Bay, Hogan Bay, Iktua Bay, Johnson Bay, and Whale Bay). The PWS samples included both gill and adductor tissue, whereas the KATM and LACL samples only included gill tissue (**Table 1**). During the 2020 LTEMP sampling event, 69 samples were collected and analyzed (**Table 1**). The transcription of the 15 genes was analyzed in all 69 samples (**Table 2**).

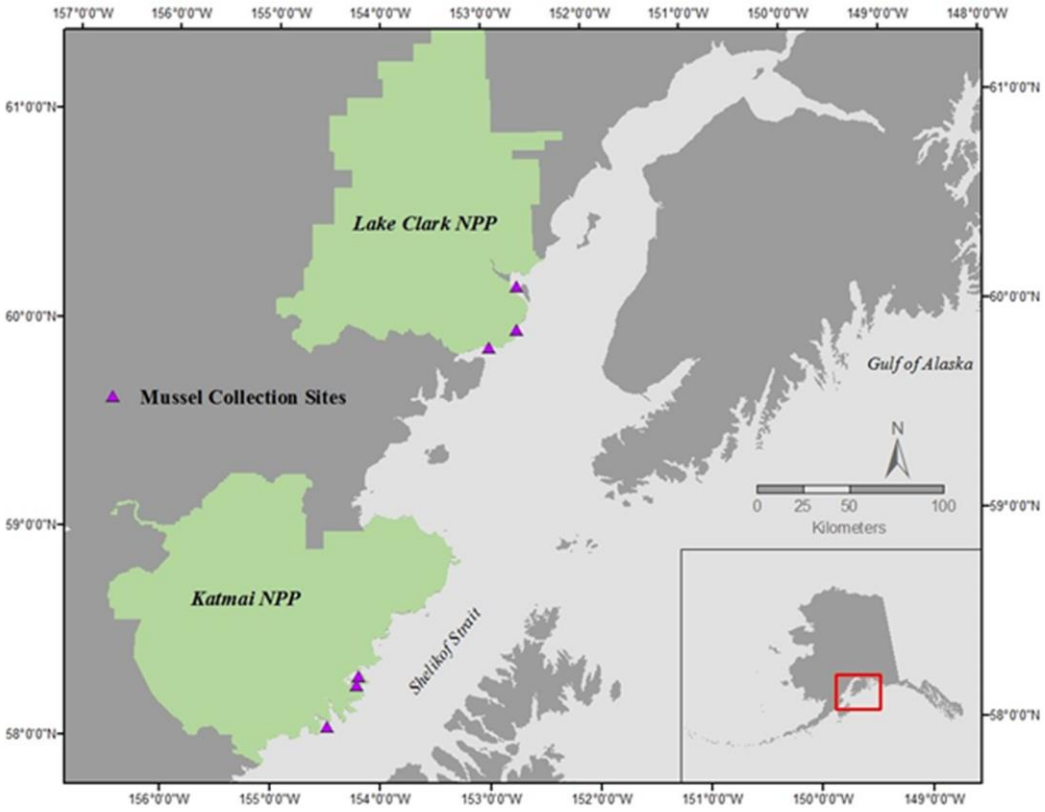

Figure 3. Mussel sampling sites in Lake Clark National Park and Preserve (NPP) and Katmai NPP. Sites were sampled during June of 2015 and 2016.

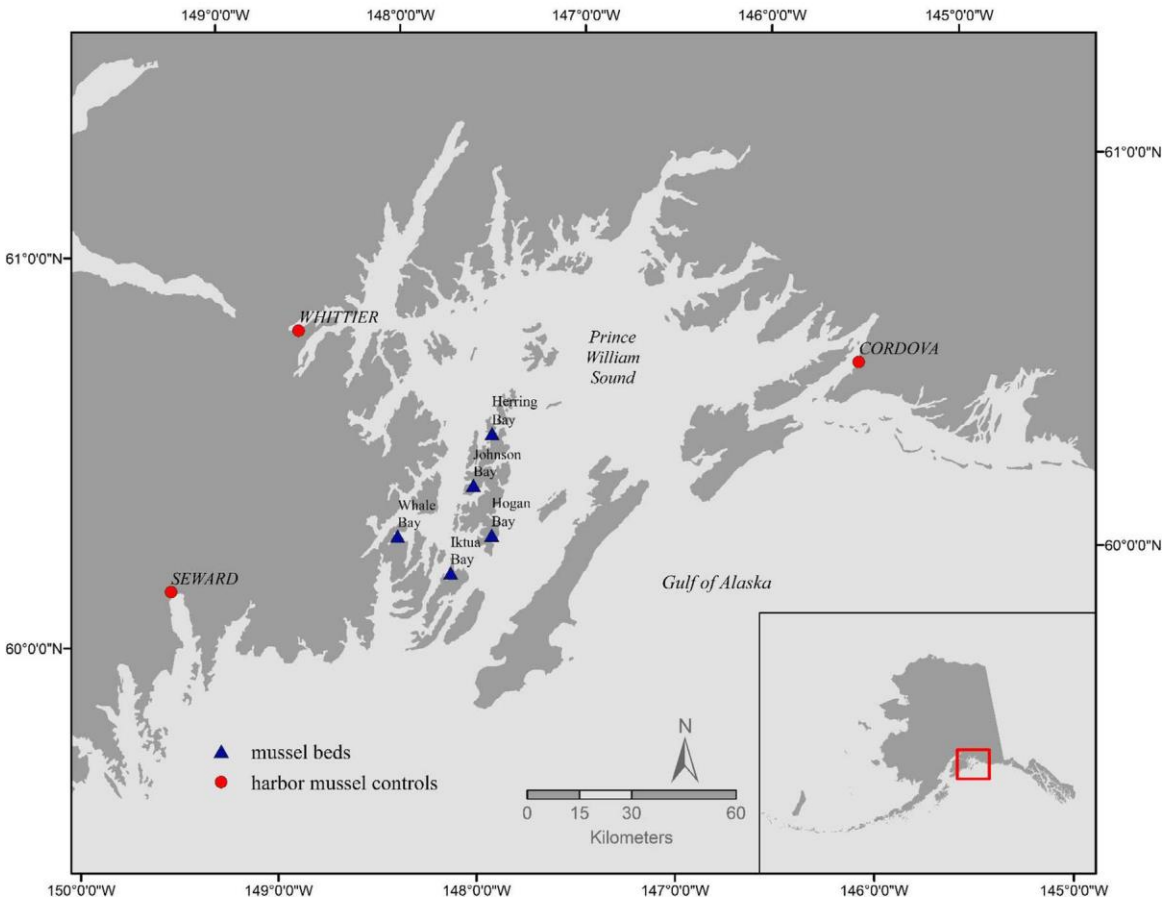

Figure 4. Location of harbor and field mussel sampling sites in Prince William Sound.

Table 1. Numbers of samples of gill and adductor muscle tissues sampled by site. KATM and LACL each include three separate sites. PWS includes five field sites and three harbor sites.

Abbreviation	Gill	Adductor	Location & Collection Year
AMT19	10	10	Saw Island 2019
AMT20	10	10	Saw Island 2020
GB20	10	10	Galena Bay 2020
GoC19	10	10	Gold Creek 2019
GoC20	10	10	Gold Creek 2020
JB20	10	10	Jack Bay 2020
JPO19	10	10	Jackson Point 2019
JPO20	10	10	Jackson Point 2020
KATM	60	0	Katmai National Park 2015-2016
LACL	60	0	Lake Clark National Park 2015-2016
PWS	23	90	Prince William Sound 2012-2015
VH19	10	10	Valdez Small Boat Harbor 2019
VH20	19	19	Valdez Small Boat Harbor 2020

Table 2. Genes selected for the transcription panel, the primary biological processes they are associated with, and what types of environmental interactions are known to affect their transcription.

Gene	Biological Process	Environmental Interaction	References
Calmodulin (CaM)	Metabolism, shell formation	Ocean acidification Temperature Dissolved oxygen	Chen et al. (2012); Li et al. (2004)
Caspase 8 (Casp8)	Programmed cell death, necrosis, inflammation	Pathogens Contaminants	Romero et al. (2011)
Macrophage migration inhibitory factor (MIF)	Innate immunity	Pathogens	Parisi et al. (2012), Philipp et al. (2012)
Calponin (CNN)	Hypoxia	Ocean acidification Dissolved oxygen	Hüning et al. (2013), Li et al. (2016)
Chitinase (CHI)	Metabolism, hypoxia	Ocean acidification Dissolved oxygen	Banni et al. (2011), Hüning et al. (2013)
Cytochrome C Oxidase IV (CCOIV)	Hypoxia	Dissolved oxygen	Fukuda et al. (2007)
Heat shock protein 70 (HSP70)	Thermal stress	Temperature, Pathogens, Contaminants	De Maio (1999), Iwama et al. (1999), Tsan & Gao (2004)
Heat shock protein 90 (HSP90)	Thermal stress	Temperature Pathogens Contaminants	De Maio (1999), Iwama et al. (1999), Tsan & Gao (2004)
Hypoxia-inducible factor alpha (HIFa)	Hypoxia	Dissolved oxygen	Wu (2002)
Myticin B (MytB)	Innate immunity	Pathogens	Balseiro et al. (2011)
Mytilin (Myt)	Innate immunity	Pathogens Ocean acidification	Balseiro et al. (2011), Mitta et al. (2000)
Metallothionein 20 (MT20)	Detoxification	Contaminants - metals	Banni et al. (2007)
Cytochrome P450, family 3 (Cyp3)	Detoxification	Contaminants	Giuliani et al. (2013)
Tumor protein 53 (P53)	Programmed cell death	Contaminants - PAHs	Goodson et al. (2006), Banni et al. (2009)
Ribosomal 18S (18S)	Method reference gene	Low interaction potential	Counihan et al. 2019

RNA extraction

Total RNA was extracted from homogenized adductor muscle and gill tissue using the RNeasy Lipid Tissue Mini Kit (Qiagen, Valencia, CA). To remove contaminating genomic DNA, the spin columns were treated with 10 U μL^{-1} of RNase-free DNase I (DNase, Amersham Pharmacia Biotech Inc.; www.apbiotech.com) at 20 °C for 15 minutes (min) followed by extraction of total RNA and stored at −80 °C.

cDNA synthesis

A standard complementary deoxyribonucleic acid (cDNA) synthesis was performed on 2 µg of RNA template from each tissue. Reaction conditions included 4 units reverse transcriptase (Omniscript, Qiagen, Valencia, CA), 1 µM random hexamers, 0.5 mM each dNTP, and 10 units RNase inhibitor, in RT buffer (Qiagen, Valencia, CA). Reactions were incubated for 60 min at 37 °C, followed by an enzyme inactivation step of 5 min at 93 °C, and then stored at –30 °C until further analysis. Real-time polymerase chain reaction (PCR) reactions for the individual, mussel-specific housekeeping gene (18S) and genes of interest were run in separate wells (**Table 2**).

Briefly, 1 µl of cDNA was added to a mix containing 12.5 µl of Applied Biosystems Fast SYBR Green® Master Mix [5 mM Mg2+] (Qiagen, Valencia, CA), 0.5 µl each of forward and reverse sequence specific primers (Invitrogen, Carlsbad, CA), and 10.5 µl of RNase-free water; total reaction mixture was 25 µl. The reaction mixture cDNA samples for each gene of interest and 18S were loaded into Fast SYBR Green® 96 well plates in duplicate and sealed with optical sealing tape (Applied Biosystems, Foster City, CA). Reaction mixtures that contained water but no cDNA were used as negative controls. Amplifications were conducted on a Step-One Plus Real-time Thermal Cycler (Applied Biosystems, Foster City, CA). Reaction conditions were as follows: 50 °C for 2 min, 95 °C for 15 min, 40 cycles of 94 °C for 30 seconds (s), 60 °C for 30 s,

72 °C for 31 s, and an extended elongation phase at 72 °C for 10 min. Reaction specificity was monitored by melting curve analysis using a final data acquisition phase of 60 cycles of 65 °C for 30 s and verified by direct sequencing of randomly selected amplicons. Cycle threshold crossing values (C_T) for the genes of interest were normalized to the 18S housekeeping gene. The C_T value of a reaction is defined as the PCR cycle number when the fluorescence of a PCR product can be detected above the background signal and is associated with the amount of PCR product in the reaction. Thus, the lower the C_T value, the more PCR product that is present.

Statistical analysis

Separate statistical analyses were conducted for the two tissue types, adductor muscle and gill. Transcriptomic responses to stress are likely related to the specific physiological role of each tissue in the organism (Kadota et al. 2003) and thus, generally tissue specific. Analysis of quantitative PCR data was conducted using normalized values (ribosomal housekeeping gene threshold crossing subtracted from the gene of interest's threshold crossing). Note that while lower normalized values are indicative of higher numbers of transcripts, we have inverted the values in the box plots for ease of interpretation. A change in normalized value of two is approximately equivalent to a four-fold change in the amount of the transcript. The measured gene expression variation between samples is the sum of the true biological variation and several confounding factors (e.g., method limit differences in pipetting volume or sample adhesion to plastic wells, etc.) resulting in non-specific variation. The goal of normalization is to remove the non-biological variation as much as possible.

For descriptive analysis, median transcript values were calculated for each tissue at each location (**Table 3 and Table 4 in APPENDIX**). Tissues were analyzed individually, not as composites, and data are generally represented by site medians. Medians were used to avoid the

effects of outliers, which are kept in the data as they convey important information. Correlations between genes were calculated using a Pearson correlation matrix with heat map visualization (NCSS© Statistical Software, 2007, Kaysville, Utah).

Conventional median responses per group (based on location) were assessed for statistical significance between classification ranks using Kruskal-Wallis with Dunns' Multiple Comparison Tests and Bonferroni correction, with reported Z values (NCSS© Statistical Software, 2007, Kaysville, Utah). The 2019 and 2020 LTEMP sites mussel adductor and gill tissue samples were compared separately by location. Another analysis grouped the 2019 LTEMP adductor muscle samples and the 2020 LTEMP adductor muscle samples to then compare them with the median of the PWS adductor samples. The 2019 and 2020 LTEMP gill tissue samples were compared with mussel gill samples collected in 2015 and 2016 at KATM and LACL, as well as with samples collected in 2012-2015 in PWS.

We constructed three-dimensional scatter plots to visualize transcript levels by the various genes, tissue type, location, and year (Miner 3D ENTERPRISE, Paris, France). The 3-D graphical representations show median transcript levels by location clustered by similarity in transcription and not by pre-defined groups. Similar transcript levels group closer together in three-dimensional space.

RESULTS

Median responses

Median CT values for genes of interest for mussel adductor and gill tissues were calculated based on location and year (**Table 3 and Table 4 in APPENDIX**). Note that smaller values indicate greater levels of transcription. For comparison, median responses are depicted from mussels sampled at the complied PWS sites (field and harbors), as well as KATM and LACL (Bowen et al. 2018, Counihan et al. 2019).

Correlations

The Pearson correlation coefficient, r, can take a range of values from +1 to -1 where a value of 0 indicates that there is no association between the two variables and a value closer to +1 or -1 indicates a stronger association. Values greater than 0 indicate a positive association (as the value of one variable increases, so does the value of the other variable), while values less than 0 indicate a negative association (as the value of one variable increases, the value of the other variable decreases). Heat maps were generated for the correlation matrices for adductor and gill (**Figure 5** and **Figure 6**). Note that the rows and columns are sorted in the order suggested by hierarchical clustering. This plot graphically associates various "like" subsets of the variables that seem to be highly correlated within the subset. For example, adductor muscle tissues show no negative (blue) correlations, while for gill tissue, there are slight negative (light blue) correlations.

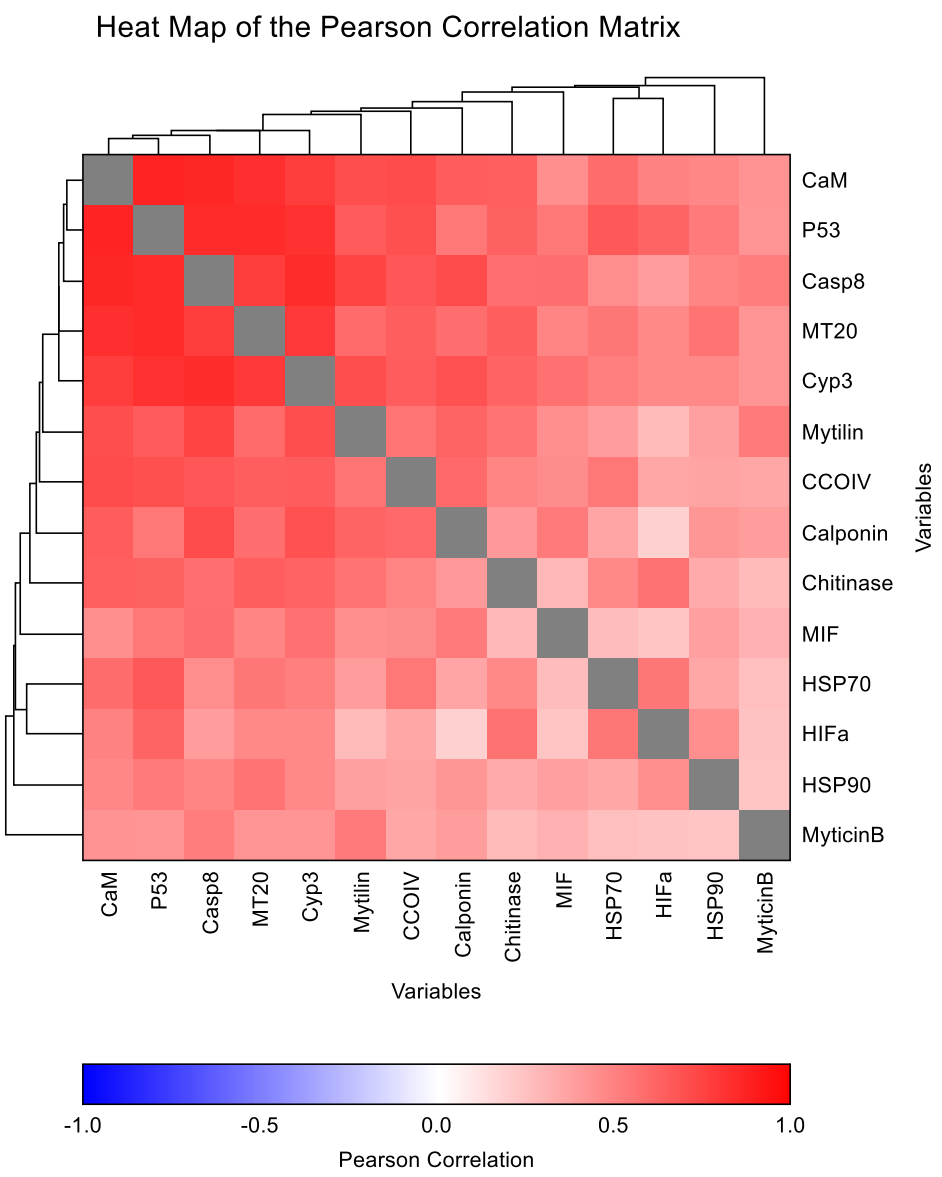

Figure 5. Heat map of LTEMP adductor muscle tissue correlation matrix

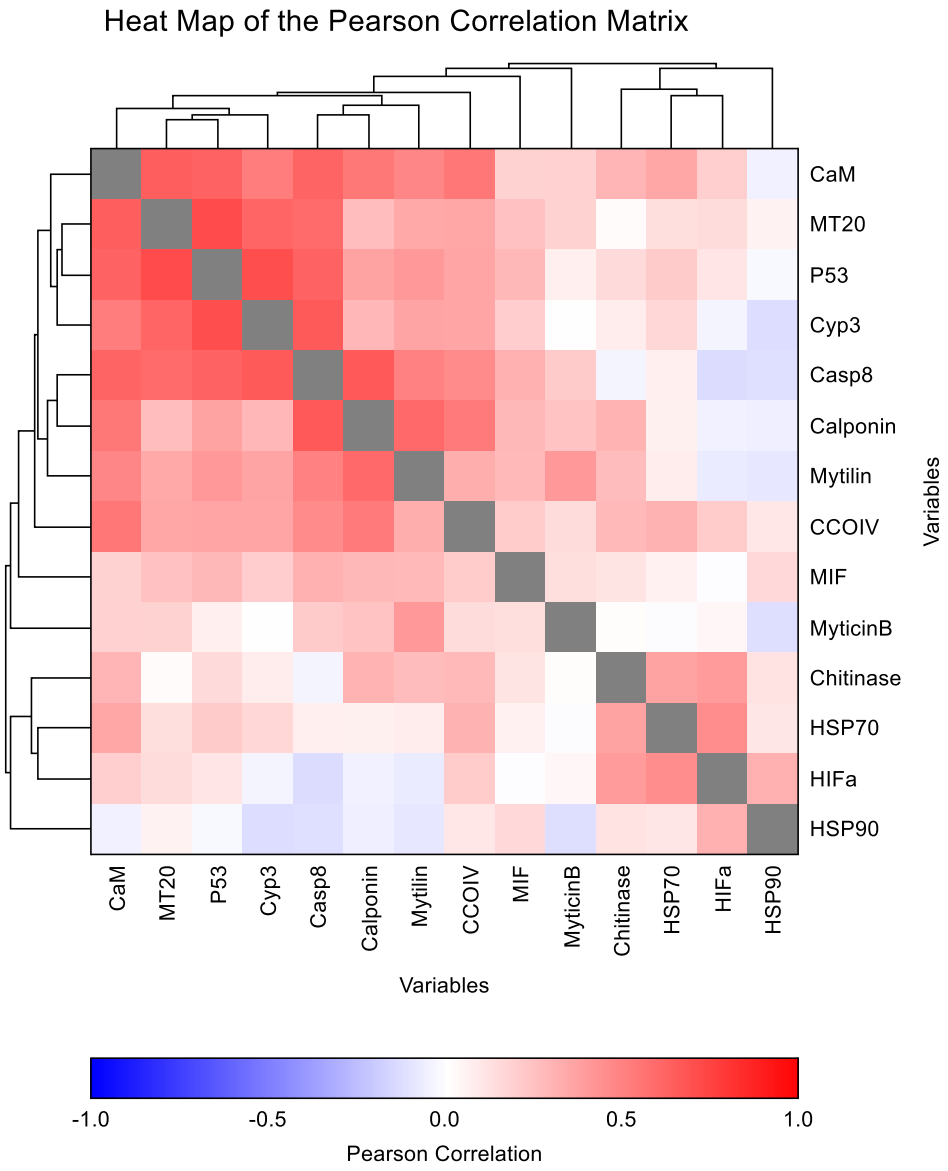

Figure 6. Heat map of LTEMP gill tissue correlation matrix

Considerations for adductor and gill tissue results

Transcriptional patterns are generally tissue specific. These tissue-specific responses are likely related to the specific physiological role of each tissue in the mussel, a phenomenon that has been found in many studies. Additionally, it has been hypothesized that the specialized functions of different tissues could make some tissues more or less susceptible to disruptions

from contaminant exposure. Thus, we have chosen to examine both gill and adductor muscle tissues for breadth of understanding.

For both adductor muscle and gill tissues, the next analyses were focused on the three genes most directly linked with response to hydrocarbon exposures, MT20, Cyp3, and P53. For both adductor and gill tissue, gene transcript levels associated with contaminant presence that were significantly different among locations included MT20, Cyp3, and P53. Although the remainder of the genes in our panel are not generally associated with detoxification, many are influenced by the presence of contaminants. For example, recent research by Banni et al. 2017, shows that controlled exposure to B[a]P results in transcriptional changes of CNN, CaM, Myt, CCOIV, and CHI. These are only a few of the indirect or "downstream" effects of contaminant exposure. The mechanism is as yet unclear, but an initiation of the detoxification pathway in this case results in effects on shell formation, mitochondrial activity, and immune function (Banni et al. 2017). In general, the 2019 and 2020 LTEMP samples, from Port Valdez and the Valdez Arm, had higher levels of transcription in genes associated with detoxification, MT20, Cyp3, and P53, than KATM, LACL, and PWS samples.

Adductor muscle tissue

The 2019 and 2020 transcript profiles of adductor tissue from Port Valdez and Valdez Arm mussels (LTEMP sites) were compared with transcript profiles from 2012 – 2015 PWS mussels. Gene transcript levels associated with contaminant presence that were significantly different among locations included MT20, Cyp3, and P53 (**Figures 7-12**). **Figure 7**, **Figure 8**, and **Figure 9** depict genes in mussel adductor tissue primarily associated with detoxification of contaminants including PAHs, compared among individual LTEMP sites (AMT, GB, GoC, JB, JPO, and VH). When sampled twice, sites were split into the 2019 and 2020 sampling years. These genes were

also compared among broader groupings of sites (LTEMP 2019, LTEMP 2020, and PWS; **Figure 10, Figure 11, and Figure 12**). The following box-and-whisker quartile plots use bars to depict the range from the 10th to the 90th percentile of individual normalized transcription values for each gene. The rectangular box indicates the 1st and 3rd quartiles around the median mid-line. Red circles, if present, represent 5th and 95th percentile outliers. Interpretation of sampling location and gene abbreviations are provided in **Table 1** and **Table 2**.

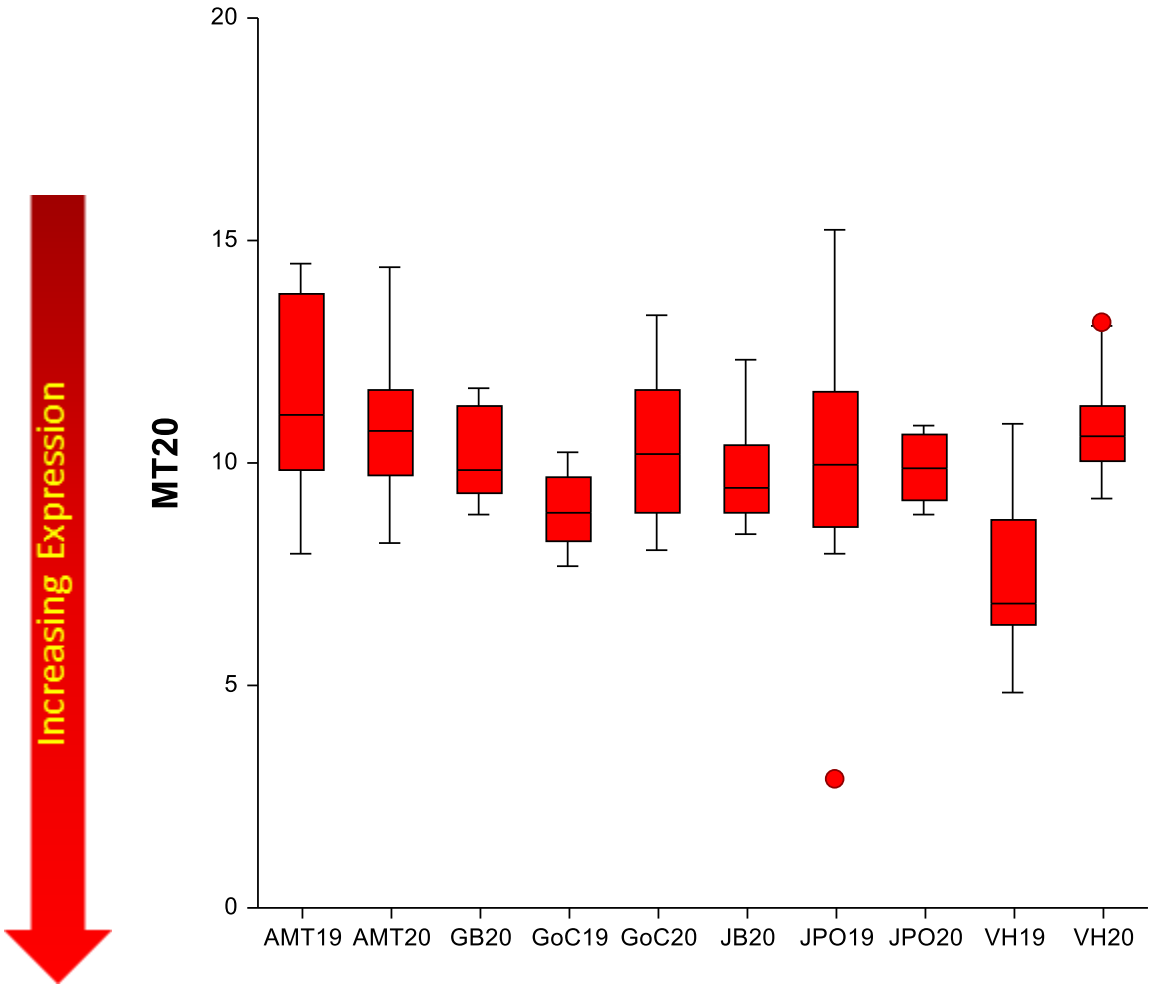

Figure 7. MT20 transcript levels in adductor muscle tissues collected as part of 2019 and 2020 LTEMP.

For MT20, indicative of hydrocarbon as well as metal exposure, the highest transcript levels in adductor muscle tissue were found in mussels sampled in VH19. Data were assessed for statistical significance between locations/years using Kruskal-Wallis with Dunns' Multiple Comparison Tests and Bonferroni correction, with reported Z values (NCSS© Statistical Software, 2007, Kaysville, Utah). ">" can be translated as "has higher transcription than." Significant differences: GoC19 > AMT19, VH20; VH19 > AMT19, AMT20, VH20 (P = 0.00).

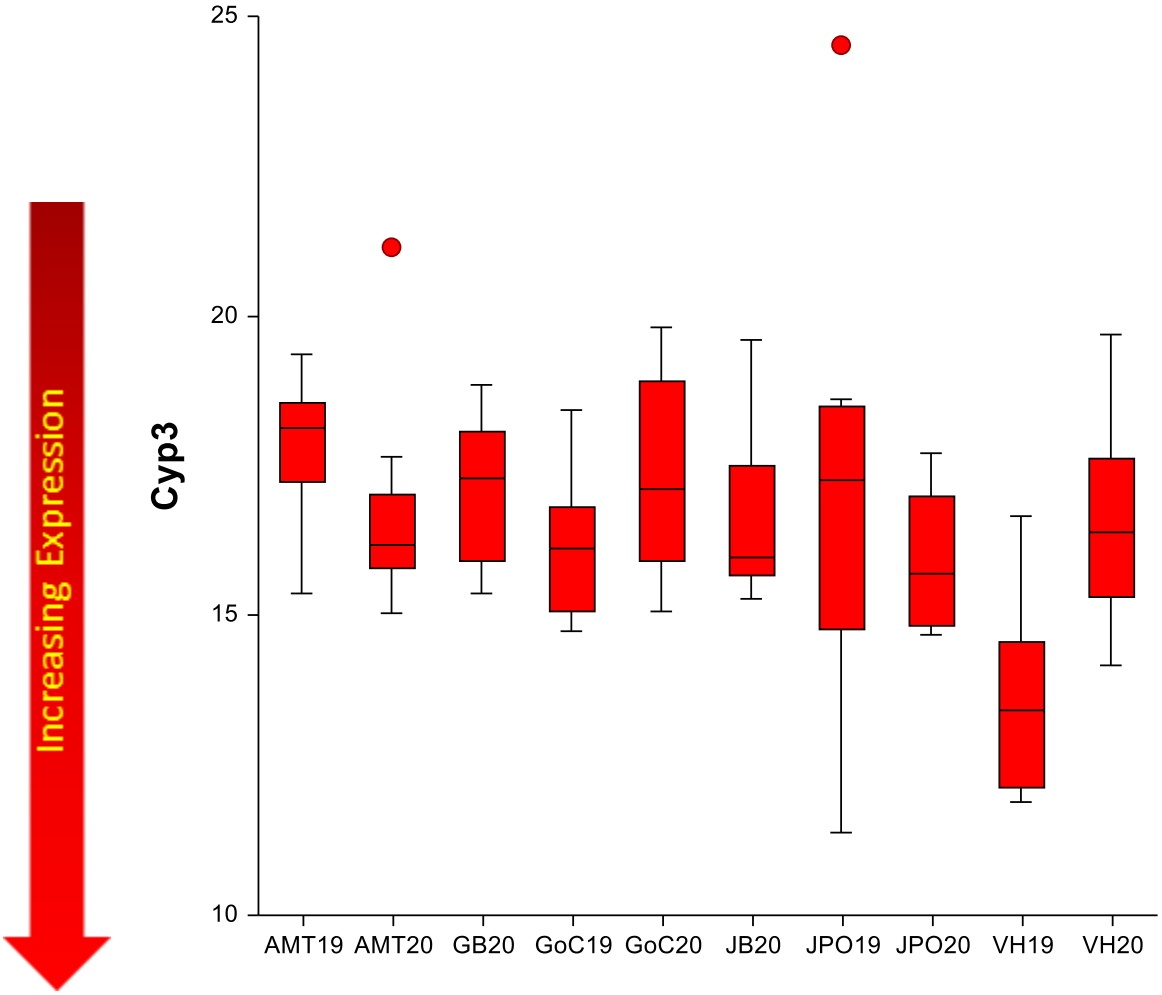

Figure 8. Cyp3 transcript levels in adductor muscle tissues collected as part of 2019 and 2020 LTEMP.

For Cyp3, indicative of contaminant detoxification activities including PAHs, the highest transcript levels in adductor muscle tissue were found in mussels sampled at VH19. Data were assessed for statistical significance between locations/years using Kruskal-Wallis with Dunns' Multiple Comparison Tests and Bonferroni correction, with reported Z values (NCSS© Statistical Software, 2007, Kaysville, Utah). ">" can be translated as "has higher transcription than." Significant differences: VH19 > AMT19, GB20, GoC20, JPO19 (P = 0.00)

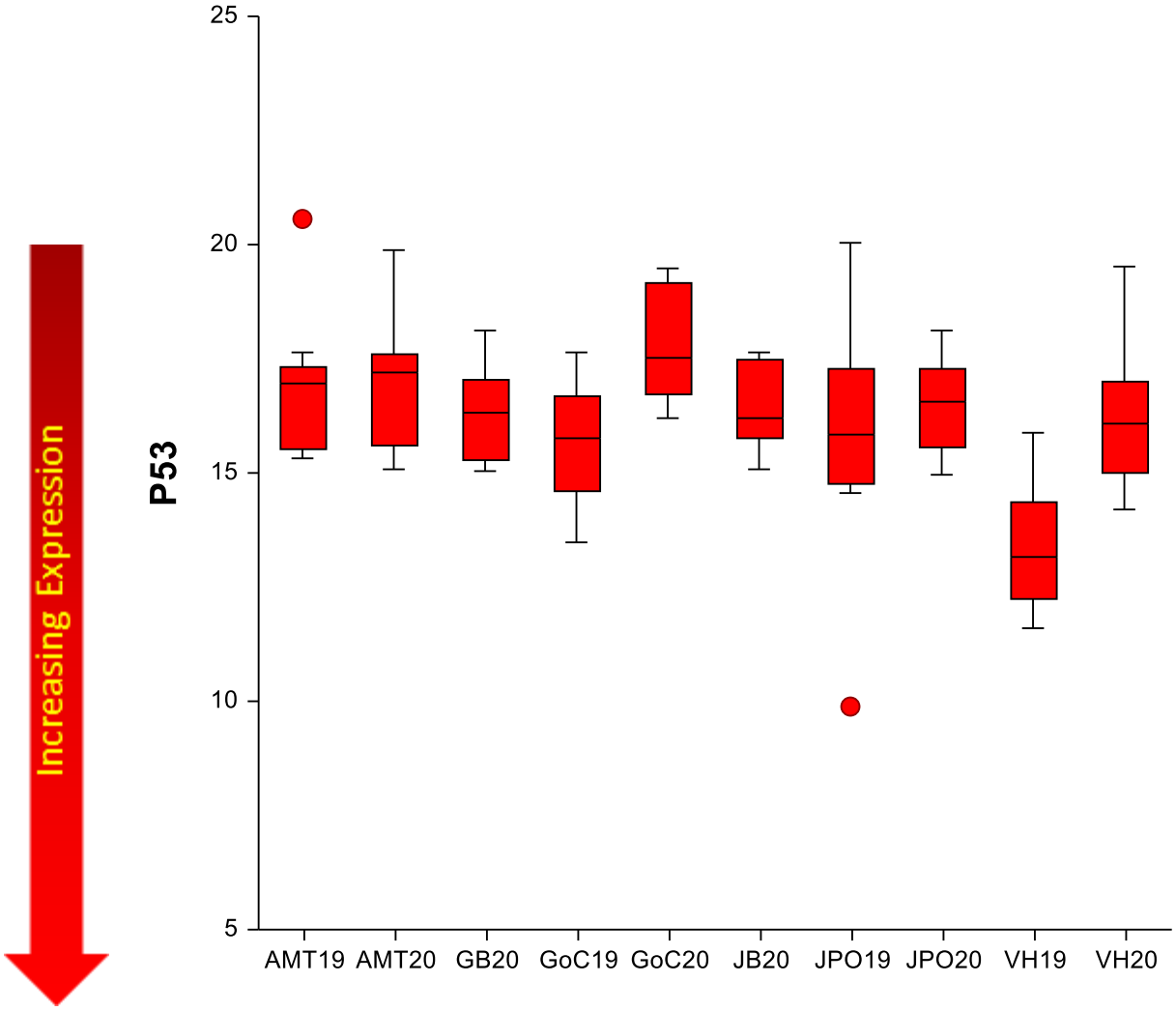

Figure 9. P53 transcript levels in adductor muscle tissues collected as part of 2019 and 2020 LTEMP.

For P53, primarily indicative of cell death and malignant transformation, as well as PAH exposure, the highest transcript levels in adductor muscle tissue were found in mussels sampled in VH19. Data were assessed for statistical significance between locations/years using Kruskal-Wallis with Dunns' Multiple Comparison Tests and Bonferroni correction, with reported Z values (NCSS© Statistical Software, 2007, Kaysville, Utah). ">" can be translated as "has higher transcription than." Significant differences: VH19 > AMT19, AMT20, GB20, GoC20, JB20, VH20 (P = 0.00).

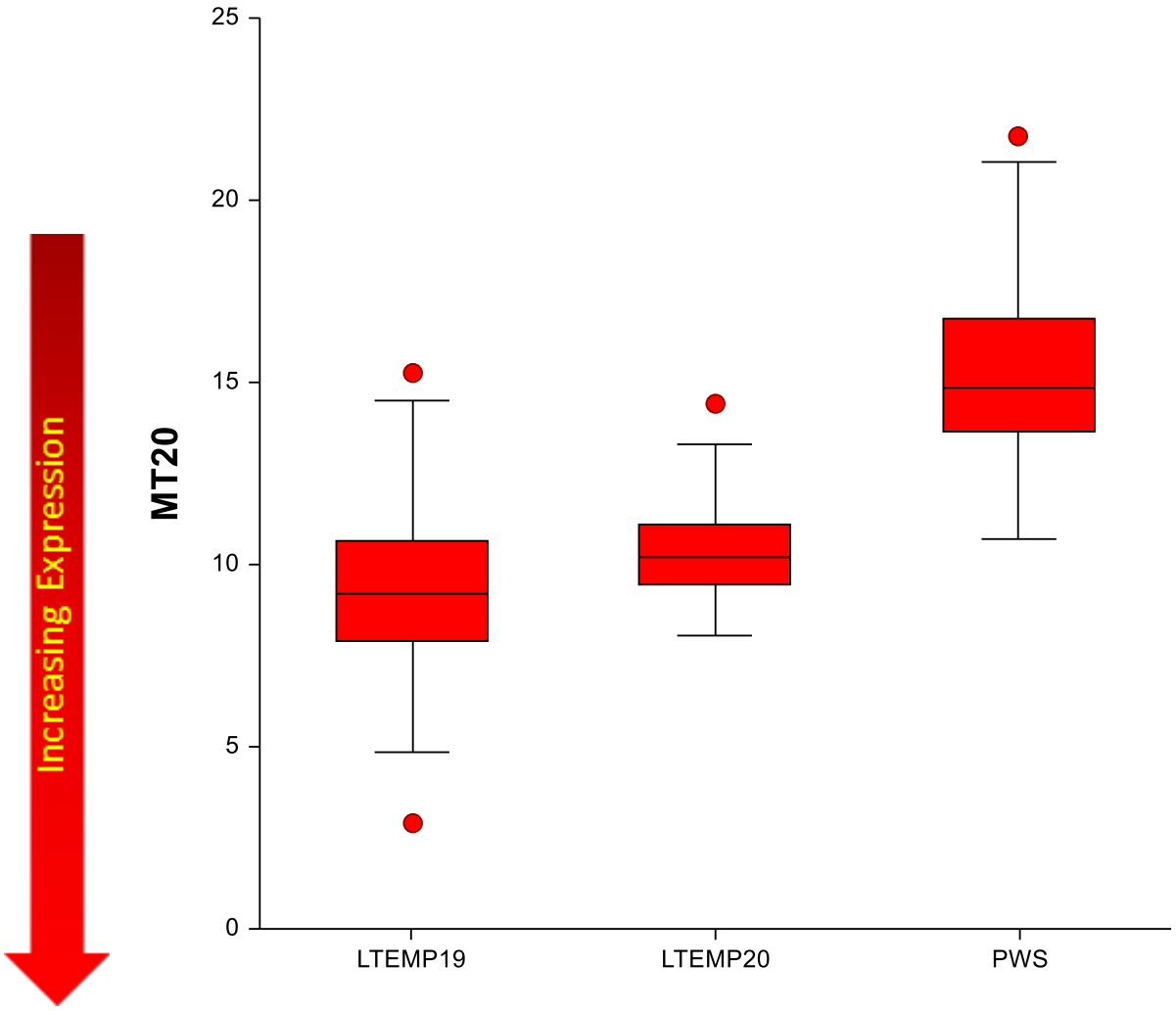

Figure 10. MT20 transcript levels in adductor muscle tissues collected as part of LTEMP 2019 and 2020, and Prince William Sound.

For MT20, indicative of hydrocarbon as well as metal exposure, the highest transcript levels in adductor muscle tissue were found in mussels sampled at the LTEMP 2019 and 2020 sites in comparison with sites in PWS (Field and Harbors). Data were assessed for statistical significance between locations/years using Kruskal-Wallis with Dunns' Multiple Comparison Tests and Bonferroni correction, with reported Z values (NCSS© Statistical Software, 2007, Kaysville, Utah). ">" can be translated as "has higher transcription than." Significant differences: LTEMP19 and LTEMP20 > PWS (P=0.00).

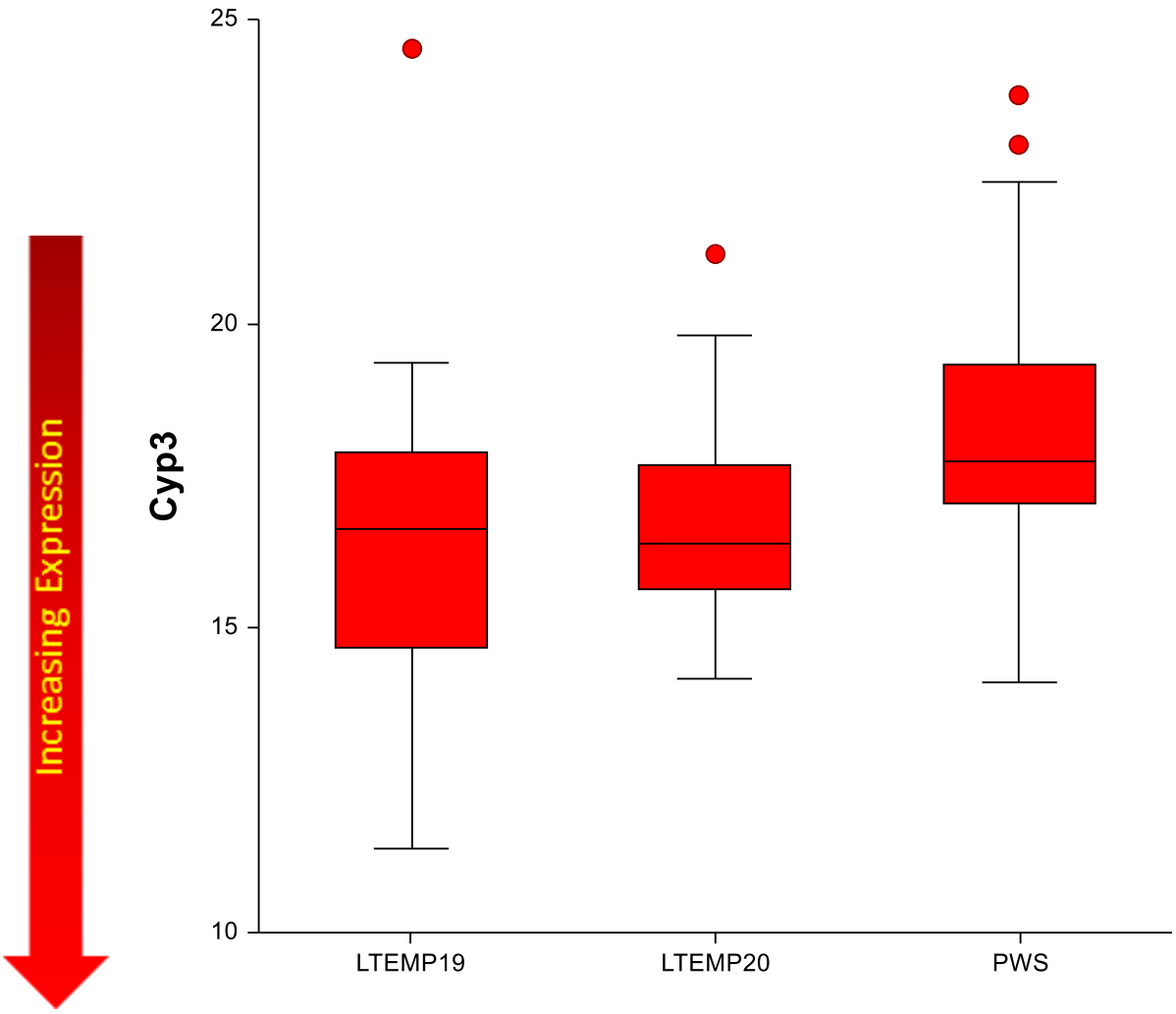

Figure 11. Cyp3 transcript levels in adductor muscle tissues collected as part of LTEMP 2019 and 2020, and PWS.

For Cyp3, indicative of contaminant detoxification activities including PAHs, the highest transcript levels in adductor muscle tissue were found in mussels sampled at the LTEMP 2019 and 2020 sites in comparison with sites in PWS (including harbors). Data was assessed for statistical significance between locations/years using Kruskal-Wallis with Dunns' Multiple Comparison Tests and Bonferroni correction, with reported Z values (NCSS© Statistical Software, 2007, Kaysville, Utah). ">" can be translated as "has higher transcription than." Significant differences: LTEMP19 and LTEMP20 > PWS (P=0.00).

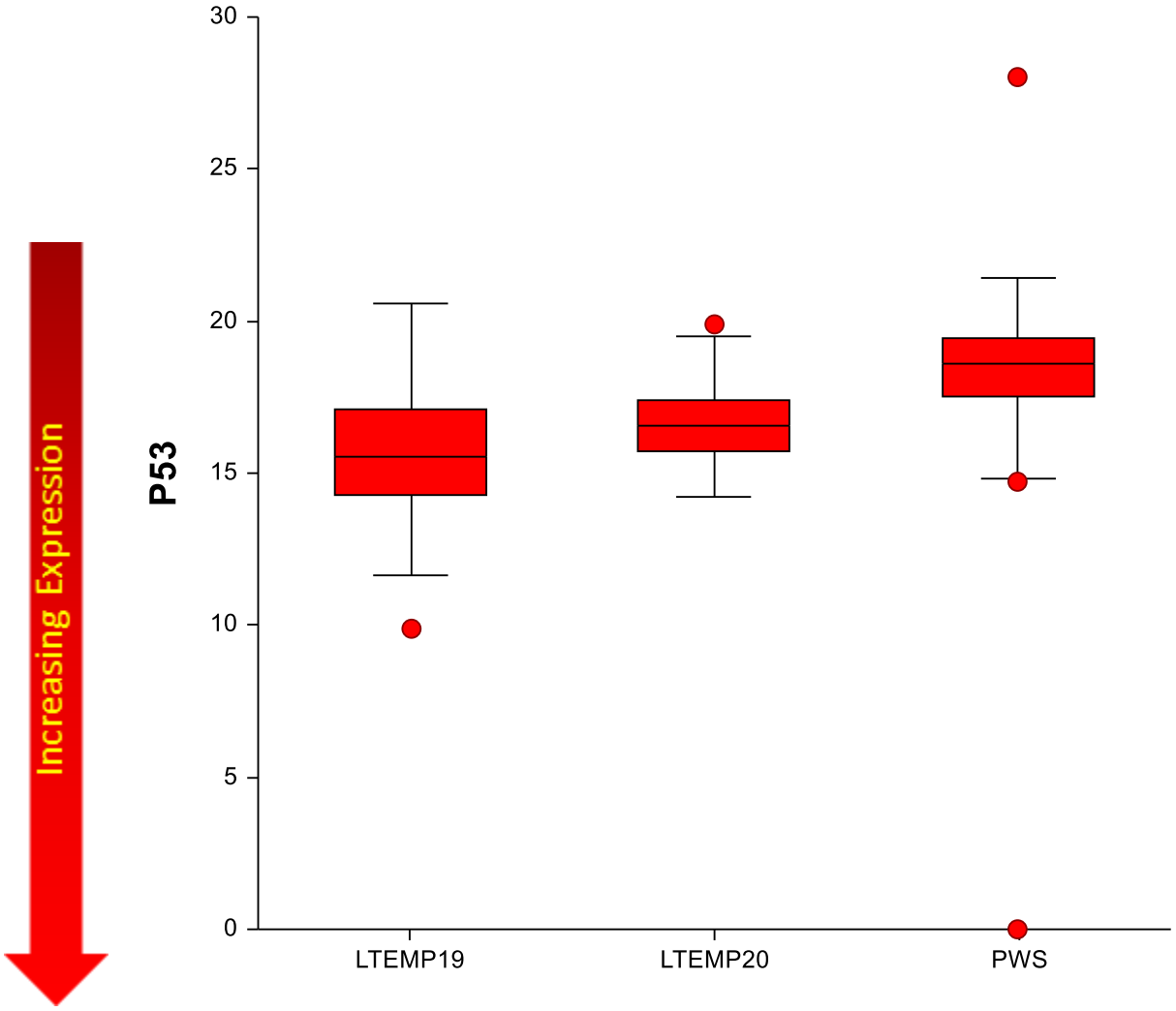

Figure 12. P53 transcript levels in adductor muscle tissues collected as part of LTEMP 2019 and 2020, and PWS.

For P53, primarily indicative of cell death and malignant transformation, as well as PAH exposure, the highest transcript levels in adductor muscle tissue were found in mussels sampled at the LTEMP 2019 and 2020 sites in comparison with sites in PWS (including harbors). Data was assessed for statistical significance between locations/years using Kruskal-Wallis with Dunns' Multiple Comparison Tests and Bonferroni correction, with reported Z values (NCSS© Statistical Software, 2007, Kaysville, Utah). ">" can be translated as "has higher transcription than." Significant differences: LTEMP19 and LTEMP20 > PWS (P=0.00).

Figure 13 and **Figure 14** depict three-dimensional scatter plots of the median values for MT20, Cyp3, and P53, in adductor tissue, at the 2019 and 2020 LTEMP sites (VH, JPO, JB, GoC, GB, and AMT) compared to the 2012-2015 PWS locations. **Figure 13** and **Figure 14** only differ in the angle of their orientation. Our results show that the highest levels of transcription of the three genes are found in mussels sampled at the VH in 2019 (black cube closest to axes origin). These samples were taken from mussels attached to a creosote piling and thus served as a strong reference for contaminant exposure. The lowest levels of transcription for each of the genes is found in mussels sampled in PWS (blue pyramid), while the remaining LTEMP samples fell in between VH19 and PWS.

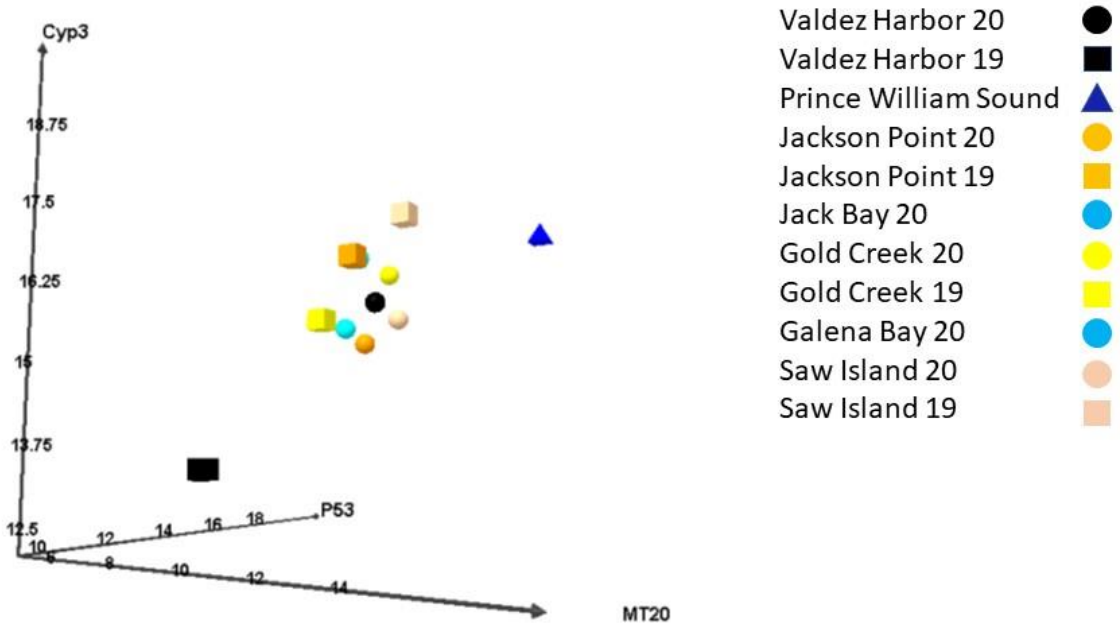

Figure 13. Three-dimensional scatter plots of the median values for MT20, Cyp3, and P53, in adductor tissue, at the 2019 and 2020 LTEMP sites (VH, JPO, JB, GoC, GB, and AMT) compared to the 2012-2015 PWS locations.

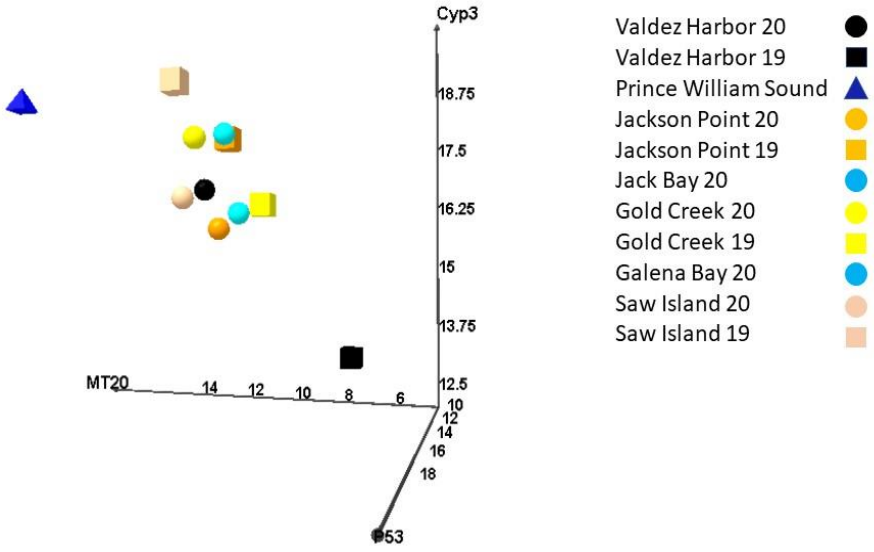

Figure 14. Three-dimensional scatter plots of the median values for MT20, Cyp3, and P53, in adductor tissue, at the 2019 and 2020 LTEMP sites (VH, JPO, JB, GoC, GB, and AMT) compared to the 2012-2015 PWS locations.

Gill tissue

The 2019 and 2020 transcript profiles of gill tissue from mussels sampled in Port Valdez and Valdez Arm (LTEMP sites) were statistically compared with transcript profiles of gill tissue from mussels sampled in LACL and KATM (collected in 2015 and 2016) and PWS (collected in 2012 – 2015). Gene transcript levels associated with contaminant presence that were significantly different among locations included MT20, Cyp3, and P53 (**Figures 15-20**). **Figure 15**, **Figure 16**, and **Figure 17** depict genes in mussel gill tissue primarily associated with detoxification of contaminants including PAHs, compared among individual LTEMP sites (AMT, GB, GoC, JB, JPO, and VH). Sites are split into sampling years (if available) 2019 and 2020. The same genes were also compared among broader groupings of sites (LTEMP 2019, LTEMP 2020, KATM and LACL) (**Figure 18, Figure 19, Figure 20**).

The following box-and-whisker quartile plots use bars to depict the range from the 10th to the 90th percentile of individual normalized transcription values for each gene. The rectangular box indicates the 1st and 3rd quartiles around the median mid-line. Red circles, if present, represent 5th and 95th percentile outliers. Interpretation of sampling location and gene abbreviations are provided in **Table 1** and **Table 2**.

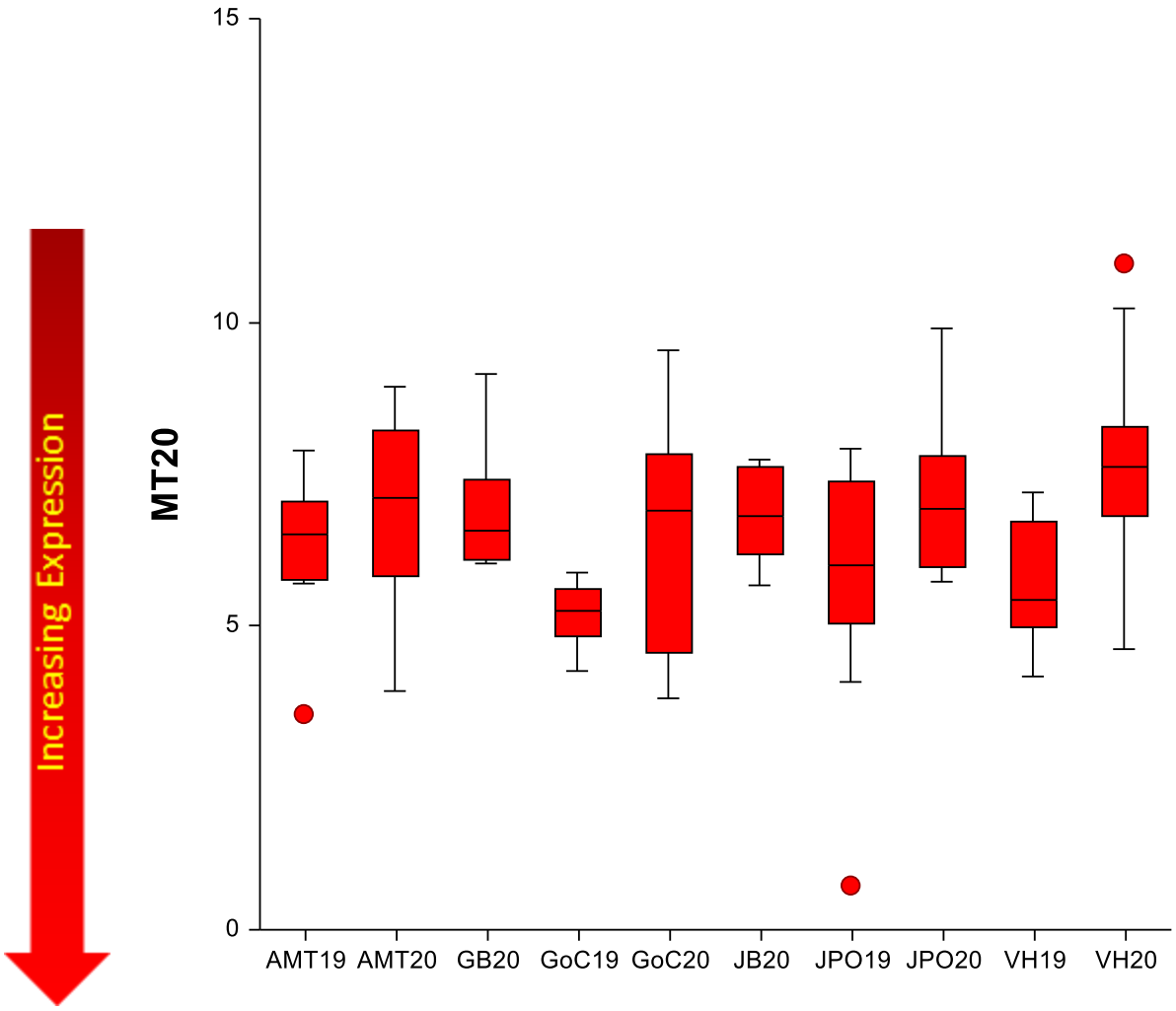

Figure 15. MT20 transcript levels in gill tissues collected as part of 2019 and 2020 LTEMP. For MT20, indicative of hydrocarbon as well as metal exposure, the highest transcript levels in gill tissue were found in mussels sampled at GoC19 and VH19. Data were assessed for statistical significance between locations/years using Kruskal-Wallis with Dunns' Multiple Comparison Tests and Bonferroni correction, with reported Z values (NCSS© Statistical Software, 2007, Kaysville, Utah). ">" can be translated as "has higher transcription than." Significant differences: GoC19 > JPO20, VH20; VH19 > VH20 (P = 0.00).

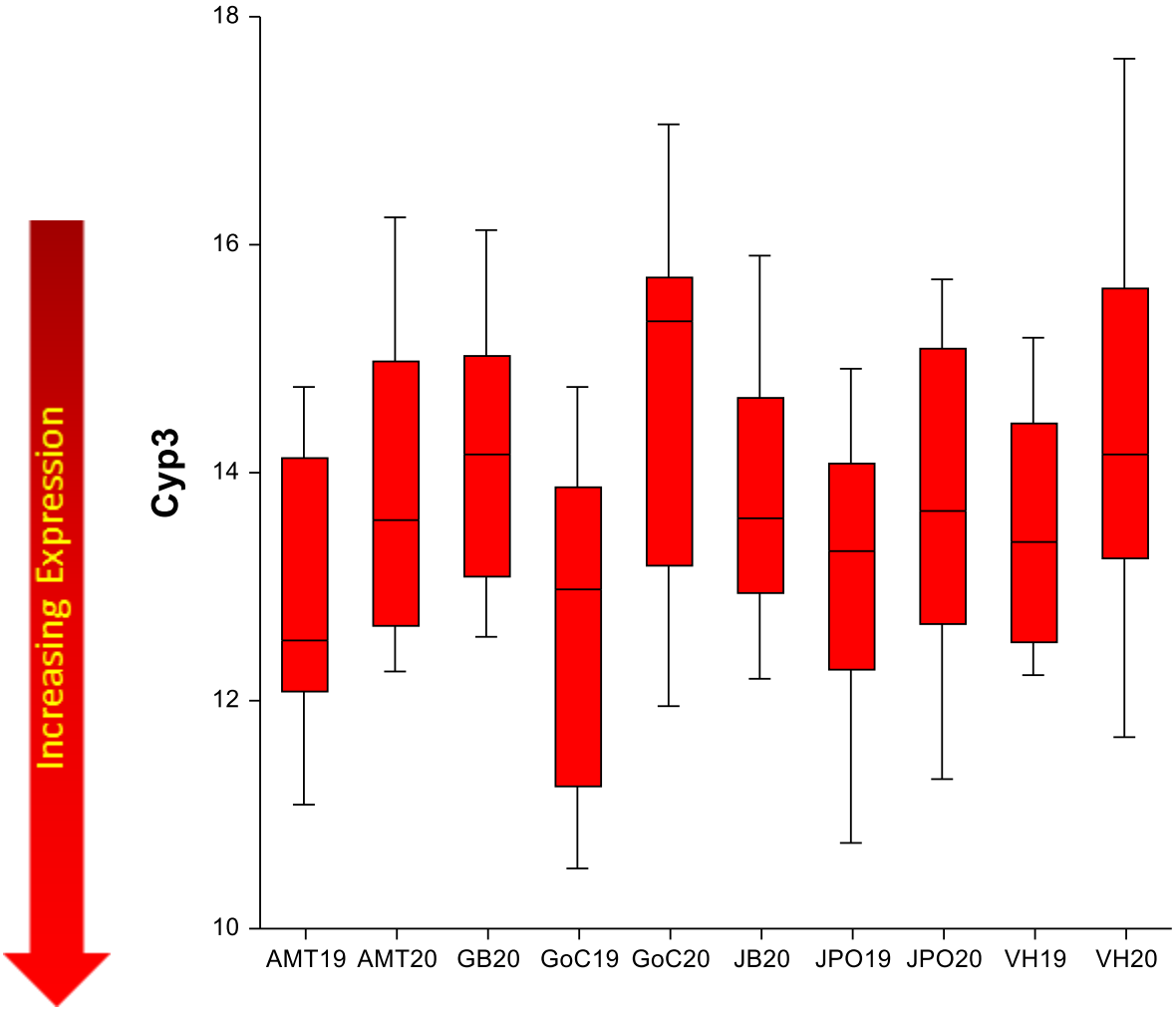

Figure 16. Cyp3 transcript levels in gill tissues collected as part of 2019 and 2020 LTEMP.

For Cyp3, indicative of contaminant detoxification activities including PAHs, the highest transcript levels in gill tissue were found in mussels sampled at AMT 2019, GoC 2019, JPO19, VH19. Data were assessed for statistical significance between locations/years using Kruskal-Wallis with Dunns' Multiple Comparison Tests and Bonferroni correction, with reported Z values (NCSS© Statistical Software, 2007, Kaysville, Utah). ">" can be translated as "has higher transcription than." Significant differences: no significant differences.

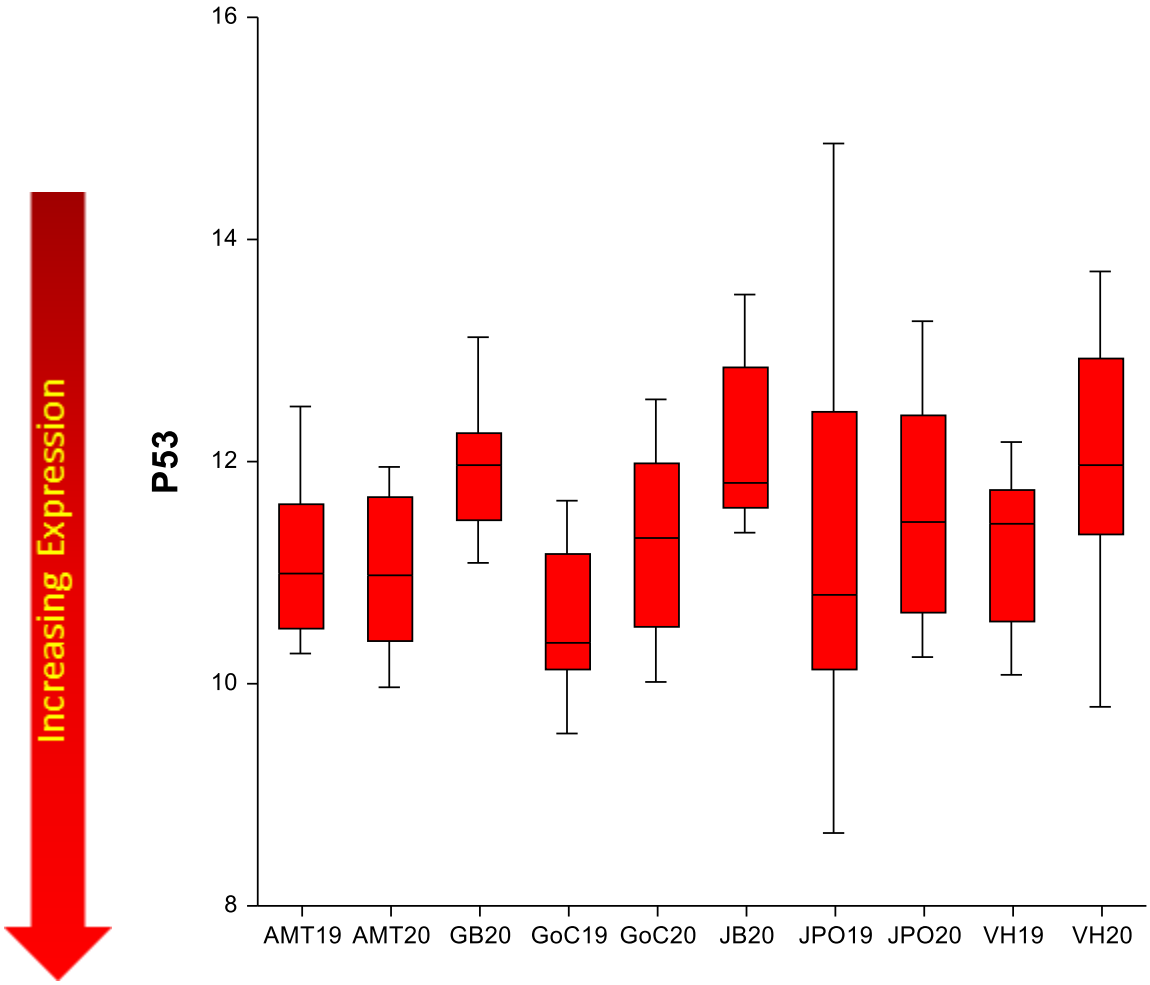

Figure 17. P53 transcript levels in gill tissues collected as part of 2019 and 2020 LTEMP.

For P53, primarily indicative of cell death and malignant transformation, as well as PAH exposure, the highest transcript levels in gill tissue were found in mussels sampled in GoC19 and JPO19. Data were assessed for statistical significance between locations/years using Kruskal-Wallis with Dunns' Multiple Comparison Tests and Bonferroni correction, with reported Z values (NCSS© Statistical Software, 2007, Kaysville, Utah). ">" can be translated as "has higher transcription than." Significant differences: GoC19 > GB20, JB20, VH20 (P = 0.00).

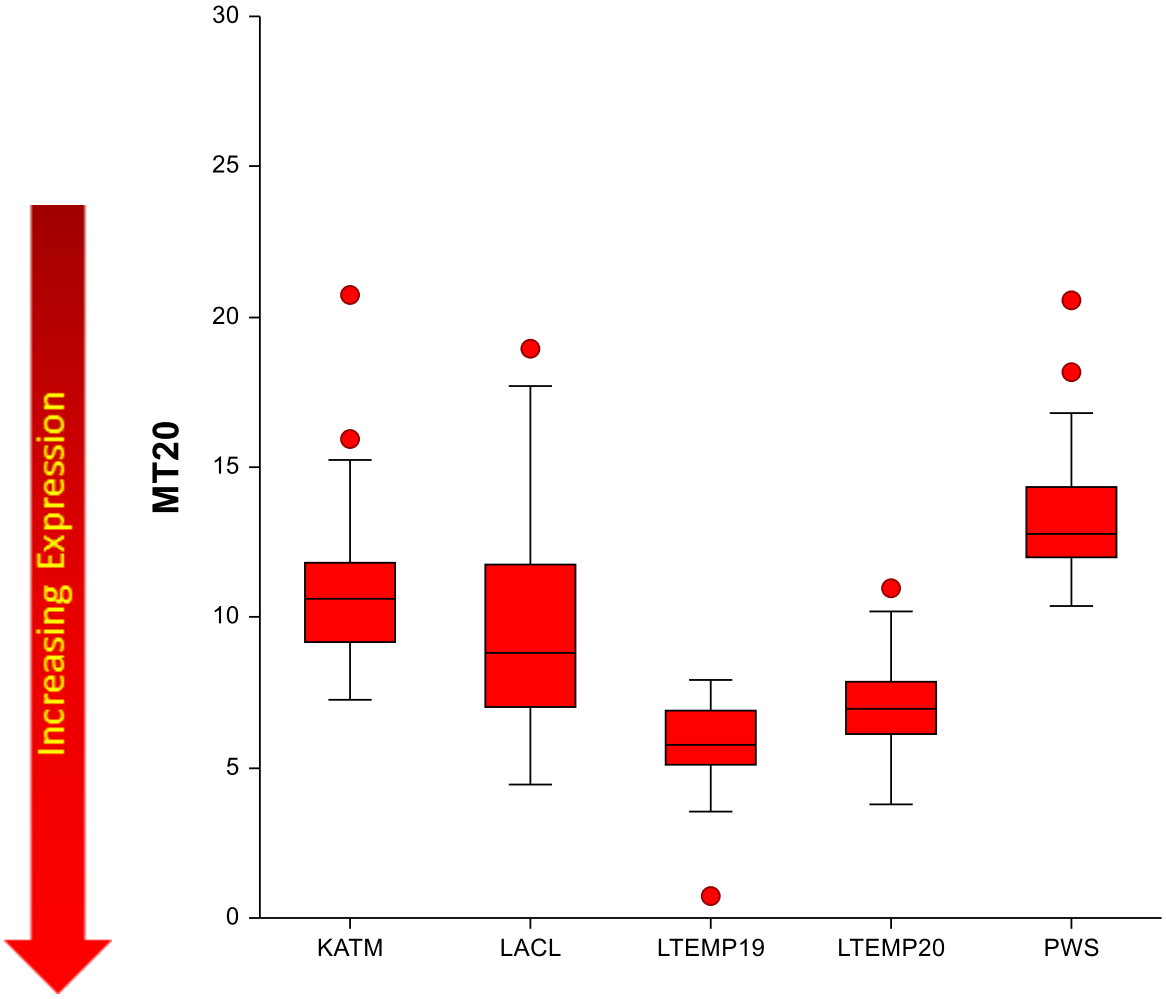

Figure 18. MT20 transcript levels in gill tissues collected as part of LTEMP 2019 and 2020, and KATM LACL, and PWS.

For MT20, indicative of hydrocarbon as well as metal exposure, the highest transcript levels in gill tissue were found in mussels sampled at the LTEMP 2019 and 2020 sites in comparison with sites in KATM, LACL, and PWS. Data were assessed for statistical significance between locations/years using Kruskal-Wallis with Dunns' Multiple Comparison Tests and Bonferroni correction, with reported Z values (NCSS© Statistical Software, 2007, Kaysville, Utah). ">" can be translated as "has higher transcription than." Significant differences: LTEMP19 > KATM, LACL, PWS; LTEMP20 > KATM, LACL, PWS; LACL > PWS (P = 0.00).

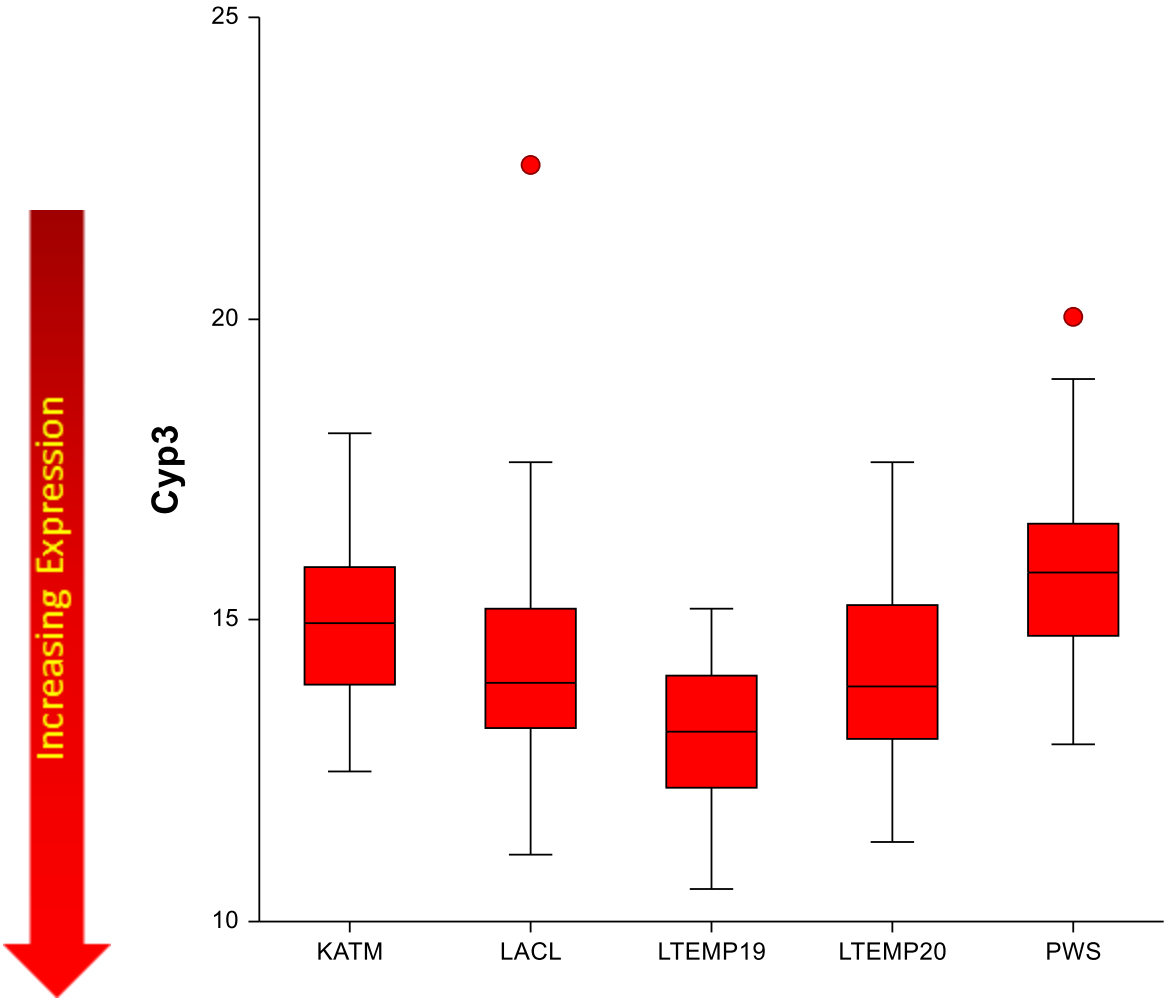

Figure 19. Cyp3 transcript levels in gill tissues collected as part of LTEMP 2019 and 2020, and KATM, LACL, and PWS.

For Cyp3, indicative of contaminant detoxification activities including PAHs, the highest transcript levels in gill tissue were found in mussels sampled at the LTEMP 2019 sites in comparison with LTEMP 2020 and sites in KATM and LACL. Data were assessed for statistical significance between locations/years using Kruskal-Wallis with Dunns' Multiple Comparison Tests and Bonferroni correction, with reported Z values (NCSS© Statistical Software, 2007, Kaysville, Utah). ">" can be translated as "has higher transcription than." Significant differences: LTEMP19 > KATM, LACL, LTEMP20, PWS; LTEMP20 > KATM, PWS; LACL > PWS (P = 0.00).

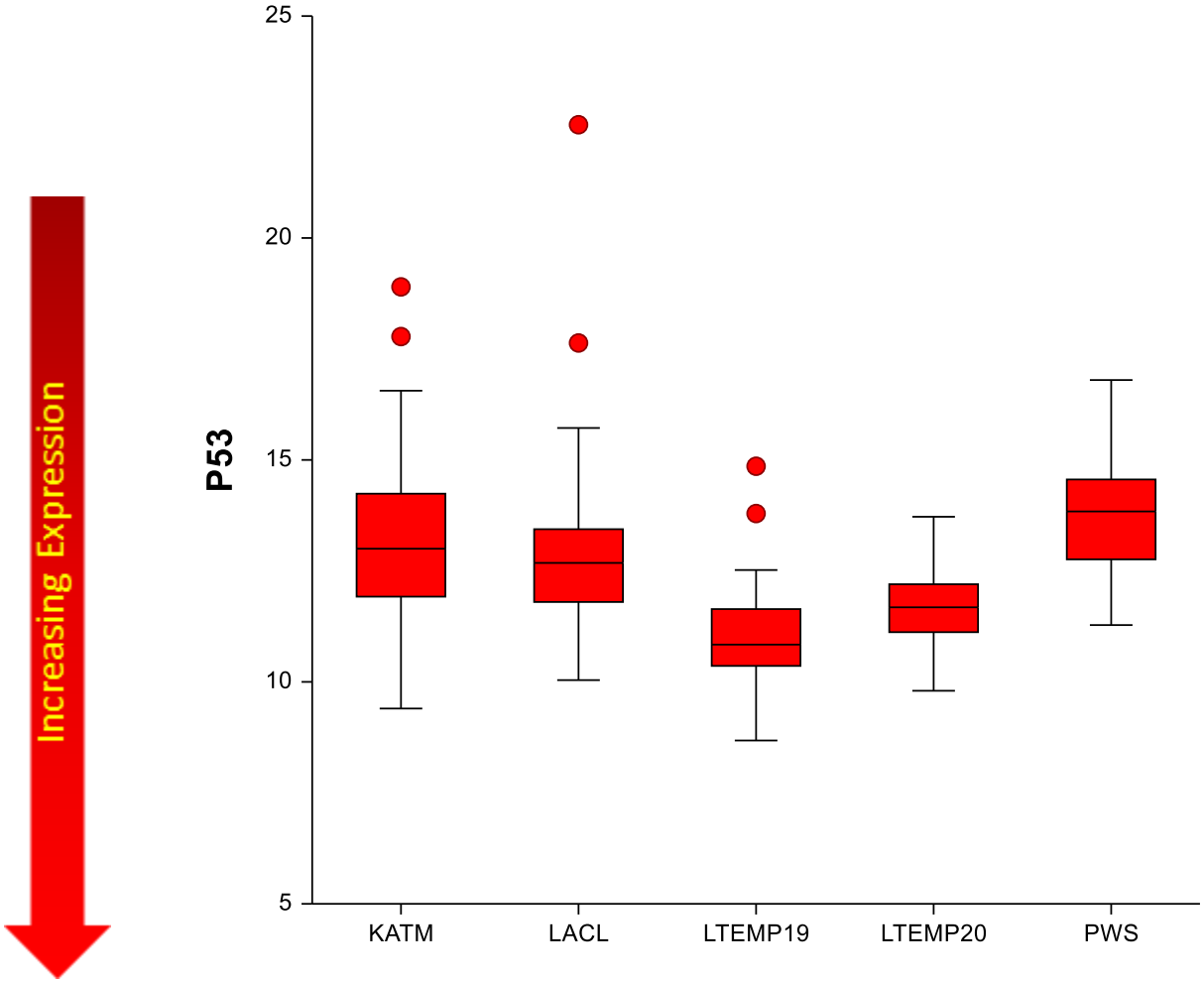

Figure 20. P53 transcript levels in gill tissues collected as part of LTEMP 2019 and 2020, and KATM, LACL, and PWS.

For P53, primarily indicative of cell death and malignant transformation, as well as PAH exposure, the highest transcript levels in gill tissue were found in mussels sampled at the LTEMP 2019 and 2020 sites in comparison with sites in KATM and LACL. Data was assessed for statistical significance between locations/years using Kruskal-Wallis with Dunns' Multiple Comparison Tests and Bonferroni correction, with reported Z values (NCSS© Statistical Software, 2007, Kaysville, Utah). ">" can be translated as "has higher transcription than." Significant differences: LTEMP19 > KATM, LACL, PWS; LTEMP20 > KATM, LACL, PWS (P = 0.00).

Three-dimensional scatter plots of the median values for MT20, Cyp3, and P53, in mussel gill tissue, form a gradient from the 2019 and 2020 LTEMP sites (VH, JPO, JB, GoC, GB, and AMT), compared to the 2012-2015 PWS, and 2015-2016 KATM and LACL samples (**Figures 21 and 22** differ only in the angle of their orientation). Our results show that the highest levels of transcription in gill tissues of the three genes are found in mussels sampled at GoC in 2019 (the yellow cube closest to the axes origin). The lowest levels of transcription for each of the genes is found in mussels sampled in PWS, LACL, and KATM (blue pyramids), while transcription of remaining LTEMP samples fell into the higher transcription range.

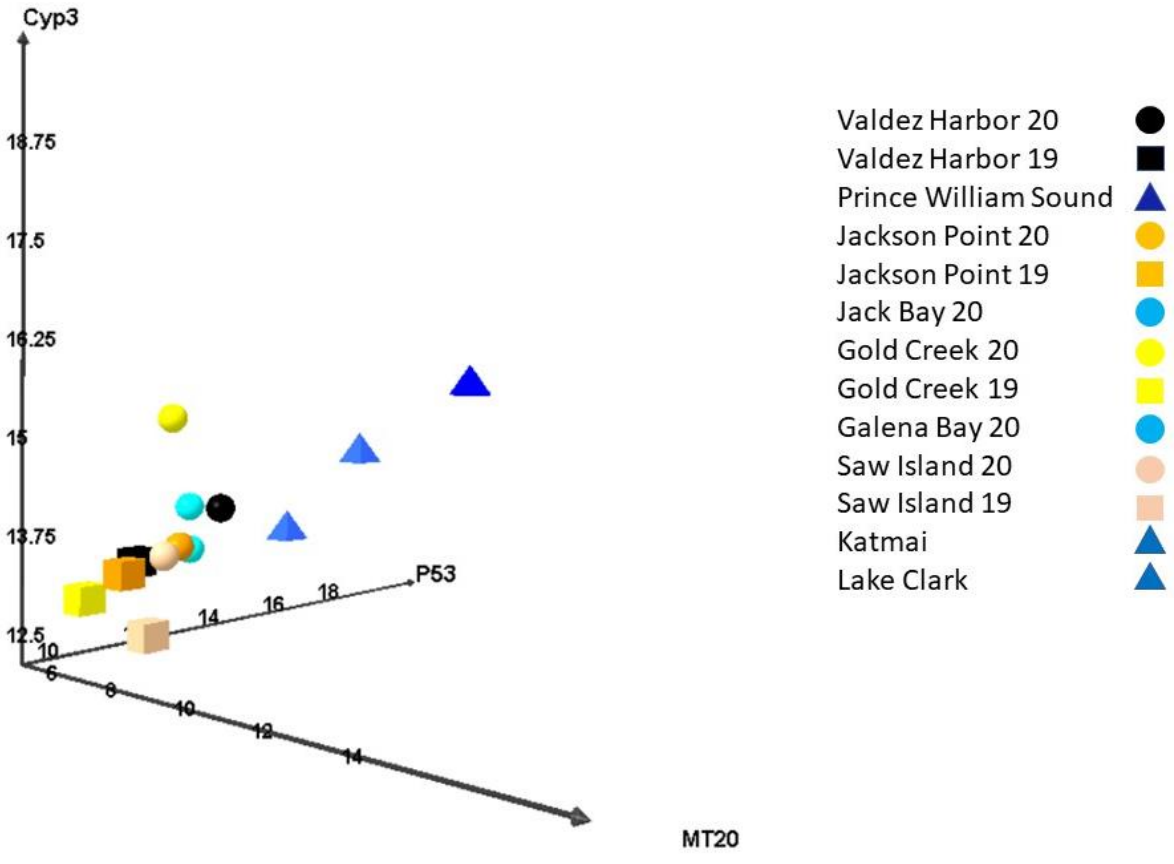

Figure 21. Three-dimensional scatter plots of the median values for MT20, Cyp3, and P53, in gill tissue, at the 2019 and 2020 LTEMP sites (VH, JPO, JB, GoC, GB, and AMT) compared to the PWS, KATM, and LACL locations.

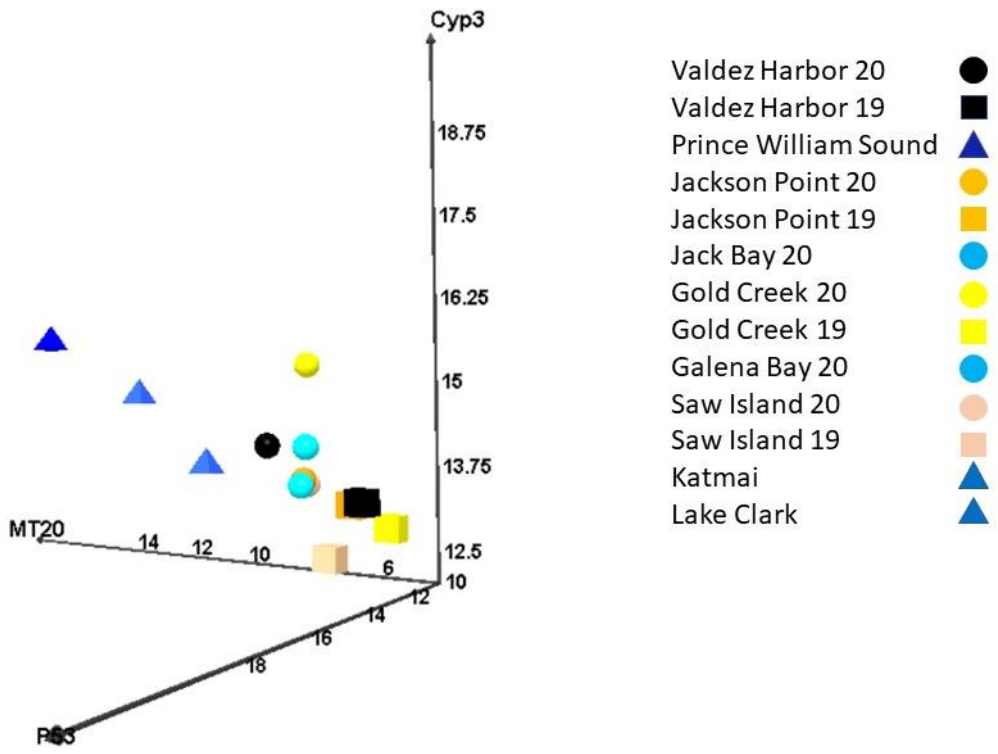

Figure 22. Three-dimensional scatter plots of the median values for MT20, Cyp3, and P53, in gill tissue, at the 2019 and 2020 LTEMP sites (VH, JPO, JB, GoC, GB, and AMT) compared to the PWS, KATM, and LACL locations.

Tissue comparison

Three-dimensional scatter plots of the median values for MT20, Cyp3, and P53, in both mussel gill and adductor tissues from the 2019 and 2020 LTEMP sites, 2012 -2015 PWS, and 2015-2016 KATM and LACL locations show similar but mostly separate response gradients (**Figure 23** and **Figure 24**). In the scatter plots, gill tissue is represented by cubes and adductor muscle tissue by spheres. Our results show that the highest levels of transcription of the three genes are found in gill tissues (cubes), although transcript levels of adductor muscles from VH19 (red sphere) group with the gill tissues. In the primarily gill cluster, the highest levels of

transcription are found in the LTEMP samples while the lowest levels are found in KATM, LACL, and PWS. In the adductor cluster (spheres), the highest transcript levels are found in the LTEMP samples (VH19 is the highest) with lowest samples seen in the PWS samples.

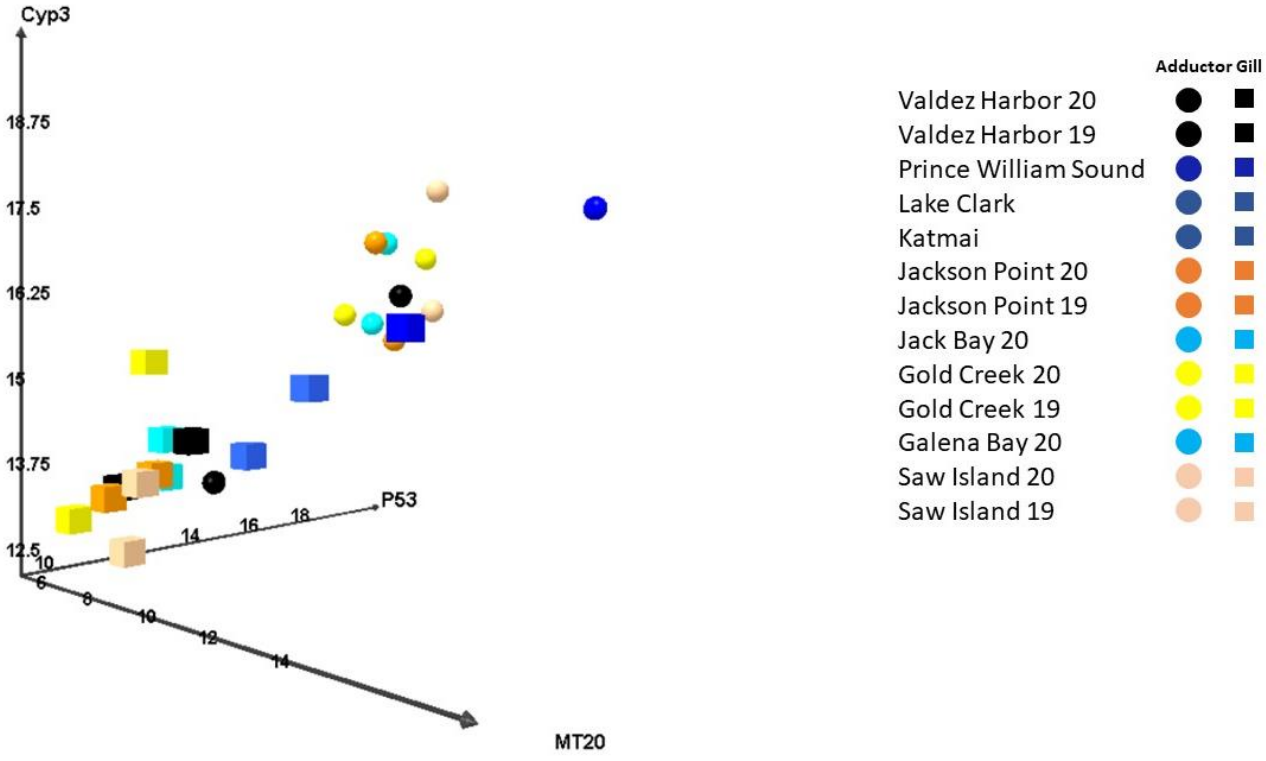

Figure 23. Three-dimensional scatter plots of the median values for MT20, Cyp3, and P53, in gill and adductor muscle tissue, at the 2019 and 2020 LTEMP sites (VH, JPO, JB, GoC, GB, and AMT) compared to the PWS, KATM, and LACL locations.

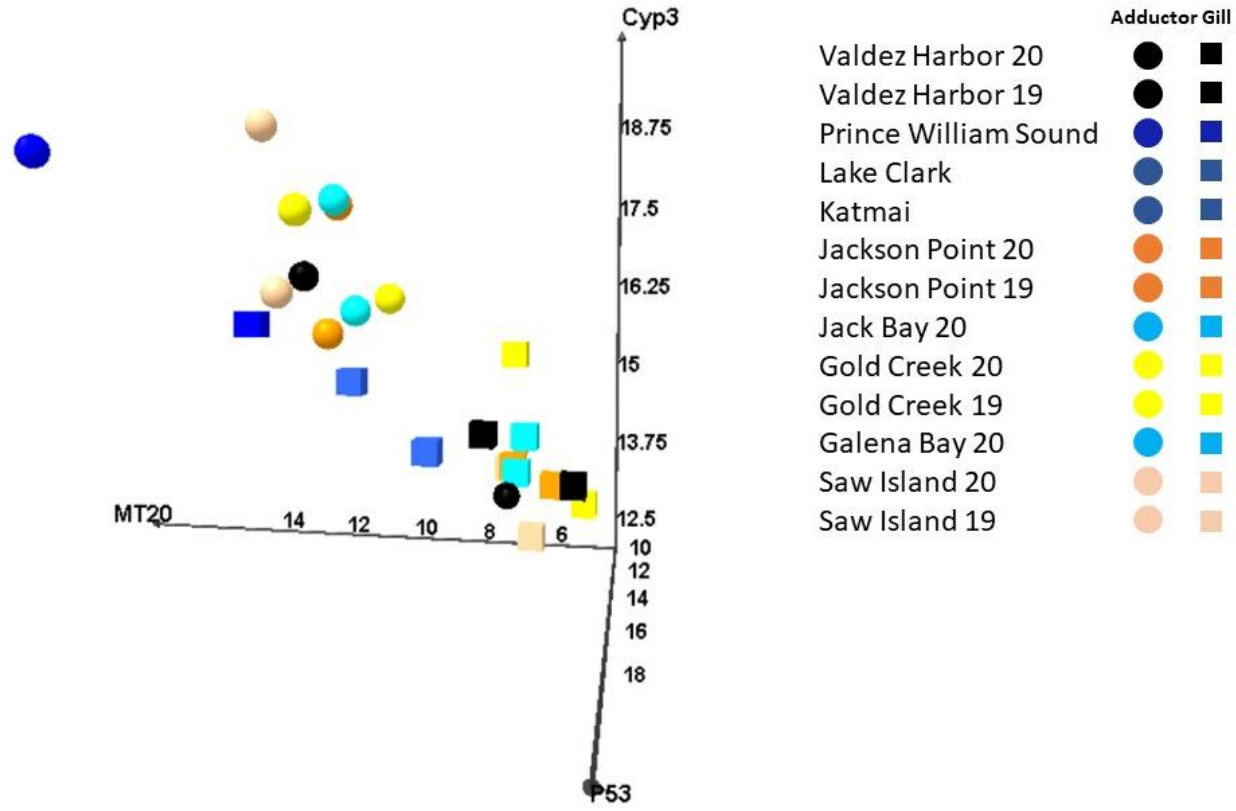

Figure 24. Three-dimensional scatter plots of the median values for MT20, Cyp3, and P53, in gill and adductor muscle tissue, at the 2019 and 2020 LTEMP sites (VH, JPO, JB, GoC, GB, and AMT) compared to the PWS, KATM, and LACL locations.

CONCLUSIONS

We have conducted a two-year analysis of gene transcription in two tissues, adductor muscle and gill, collected from mussels at four sites in Port Valdez in June 2019 and 2020 (AMT, GoC, JPO, VH) with an additional two sites in the Valdez Arm added in June 2020 to potentially act as clean reference sites (JB, GB). For comparison with these samples, we have gene expression data for mussels from sites considered to be relatively clean (for adductor muscle: western PWS Field sites, collected 2012-2015, and for gill: PWS (2012 – 2015), and KATM and LACL sites, collected 2015-2016). Additionally, we have gene expression data for

adductor tissue in mussels collected from regional harbors (Cordova, Whittier, and Seward) in 2014-2015, representing a group exposed to relatively higher levels of contaminants.

In general, for both adductor muscle and gill, our analyses indicate the expression of genes most directly associated with contaminant exposure (MT20, Cyp3, P53) was elevated in the samples from the Valdez area in 2019 and 2020 when compared to samples from "clean" sites, either in western PWS Field or in KATM and LACL. Additionally, the same gene expression was also elevated in samples from the Port of Valdez relative to other harbor sites (Whittier, Seward, and Cordova Harbor). Levels of MT20, Cyp3, and P53 transcripts increase in response to hydrocarbon exposure. These findings suggest that all six sites sampled in the Valdez area in 2019 and 2020 have levels of contaminant exposure higher than the background levels found at more remote sites in PWS, KATM, and LACL. These findings support the use of gene expression analyses in mussels as a method to monitor the presence of contaminants in Port Valdez.

RECOMMENDATIONS

1. Add at least one additional site outside Port Valdez to act as a control. When compared with expression profiles from mussels sampled in KATM, LACL, and PWS, samples from potential control sites (JB and GB) clustered with samples from the Port Valdez sites (**Figure 13, Figure 14, Figures 21-24**). This is an indication that although JB and GB may be less impacted by hydrocarbon exposure than sites closer to the Valdez Marine Terminal, they are clearly impacted more than sites in KATM, LACL, and PWS. Thus, for a broader perspective, it is recommended to add at least one and potentially two control sites chosen from sites analyzed previously (Bowen et al. 2018). These sites could potentially be sampled by Gulf Watch Alaska's environmental monitoring program crews during yearly monitoring cruises, effectively avoiding any additional field costs.

2. Assess gene transcript levels from all sites at least once per year during the same season; transcript patterns in mussels have been shown to fluctuate seasonally. However, a more robust sampling plan and design would help ensure more substantial long-term results.
3. Although overall patterns were similar, transcript profiles were tissue specific to gill and adductor muscle tissues. To get a more accurate picture of mussel responding to their environment, dual tissue sampling should continue.
4. Continue to assess hydrocarbon chemistry in mussel tissues. Current levels of hydrocarbons are below the limits of detection. As per William B. Driskell, consider adding to the existing panel of hydrocarbon chemistry analyses. It is possible that the mussels are responding physiologically to a hydrocarbon not being measured.
5. The gene transcript panel was developed prior to pilot trials for PWSRCAC and was intended to identify a broad range of stimuli. If PWSRCAC decides to include transcriptomics in future monitoring, we propose modifying this gene panel to include optimal genes specific to the needs of PWSRCAC. We propose conducting an experiment with samples from the April 12, 2020, oil spill at the Valdez Marine Terminal (already collected and in our freezer). We would perform a full transcriptome analysis (RNAseq) of mussels exposed to the spill. This would allow for identification of genes specific to the contaminants in a carefully monitored real-world spill event such as the spill from the Valdez Marine Terminal in April 2020. This will increase both the specificity and sensitivity of the gene panel for the needs of the PWSRCAC.
6. Include simple mussel morphometric measurements such as length and height in future sampling. As PWSRCAC Scientific Advisory Committee member Roger Green stated, collecting such morphometric measurements is "*not* advocating for using size, shape,

age or sex as “response to anthropogenic impact” variables; rather one should use them to control variation in impact which is in fact caused by biological variability in the animals. All we are talking about is good study design which minimizes “noise” due to factors other than the contaminants. It is similar to maintaining consistency of field and lab procedure across locations.”

REFERENCES

Balseiro P, Falcó A, Romero A, Dios S, Martínez-López A, Figueras A, Estepa A, Novoa B. 2011. Mytilus galloprovincialis Myticin C: a chemotactic molecular with antiviral activity and immunoregulatory properties. PLOS ONE 6:e23140 DOI 10.1371/journal.pone.0023140.

Banni M, Dondero F, Jebali J, Guerbej H, Boussetta H, Viarengo A. 2007. Assessment of heavy metal contamination using real-time PCR analysis of mussel metallothionein mt10 and mt20 expression: a validation along the Tunisian coast. Biomarkers 12:369_383 DOI 10.1080/13547500701217061.

Banni M, Negri A, Rebelo M, Rapallo F, Boussetta H, Viarengo A, Dondero F. 2009. Expression analysis of the molluscan p53 protein family mRNA in mussels (Mytilus spp.) exposed to organic contaminants. Comparative Biochemistry and Physiology Part C: Toxicology & Pharmacology 149:414_418 DOI 10.1016/j.cbpc.2008.09.017.

Banni M, Negri A, Mignone F, Boussetta H, Viarengo A, Dondero F. 2011. Gene expression rhythms in the mussel Mytilus galloprovincialis (Lam.) across an annual cycle. PLOS ONE 6:e18904 DOI 10.1371/journal.pone.0018904.

Banni M, Sforzini S, Arlt VM, Barranger A, Dallas LJ, Oliveri C, Aminot Y, Pacchioni B, Millino C, Lanfranchi G, Readman JW, Moore MN, Viarengo A, Jha AN. 2017. Assessing the impact of Benzo [a] pyrene on marine Mussels: Application of a novel targeted low density microarray complementing classical biomarker responses. PloS ONE 12: e0178460.

Bowen L, Miles AK, Ballachey B, Waters S, Bodkin J, Lindeberg M, Esler D. 2018. Gene transcription patterns in response to low level petroleum contaminants in Mytilus trossulus from field sites and harbors in southcentral Alaska. Deep Sea Research Part II, 147: 27-35.

Chen ZF, Wang H, Matsumura K, Qian PY. 2012. Expression of calmodulin and myosin light chain kinase during larval settlement of the barnacle Balanus amphitrite. PLOS ONE 7:e31337 DOI 10.1371/journal.pone.0031337.

Counihan K, Bowen L, Ballachey B, Coletti H, Hollmen T, Pister B. 2019. Physiological and gene transcription assays to assess responses of mussels to environmental changes. *PeerJ* 7: e7800.

De Maio AM. 1999. Heat shock proteins: facts, thoughts, and dreams. Shock 11:1_2.

Farr S, Dunn RT. 1999. Concise review: gene expression applied to toxicology. *Toxicological Sciences* 50: 1-9.

Fukuda R, Zhang H, Kim JW, Shimoda L, Dang CV, Semenza GL. 2007. HIF-1 regulates cytochrome oxidase subunits to optimize efficiency of respiration in hypoxic cells. Cell 129:111_122 DOI 10.1016/j.cell.2007.01.047.

Giuliani ME, Benedetti M, Arukwe A, Regoli F. 2013. Transcriptional and catalytic responses of antioxidant and biotransformation pathways in mussels, Mytilus galloprovincialis, exposed to chemical mixtures. Aquatic Toxicology 134_135:120_127 DOI 10.1016/j.aquatox.2013.03.012.

Goodson MS, Crookes-Goodson WJ, Kimbell JR, McFall-Ngai MJ. 2006. Characterization and role of p53 family members in the symbiont-induced morphogenesis of the Euprymna scolopes light organ. The Biological Bulletin 211:7_17 DOI 10.2307/4134573.

Heid, CA, Stevens J, Livak KJ, Williams PM. 1996. Real time quantitative PCR. *Genome Research* 6: 986-994.

Hüning AK, Melzner F, Thomsen J, Gutowska MA, Kramer L, Frickenhaus S, Rosenstiel P, Pörtner HO, Philipp EER, Lucassen M. 2013. Impacts of seawater acidification on mantle

gene expression patterns of the Baltic Sea blue mussel: implications for shell formation and energy metabolism. Marine Biology 160:1845_1861 DOI 10.1007/s00227-012-1930-9.

Iwama GK, Mathilakath MV, Forsyth RB, Ackerman PA. 1999. Heat shock proteins and physiological stress in fish. American Zoology 39:901_909 DOI10.1093/icb/39.6.901.

Kadota K, Nishimura SI, Bono H, Nakamura S, Hayashizaki Y, Okazaki Y, Takahashi K. 2003. Detection of genes with tissue-specific expression patterns using Akaike's information criterion procedure. *Physiological Genomics* 12: 251-259.

Li S, Xie L, Zhang C, Zhang Y, Gu M, Zhang R. 2004. Cloning and expression of a pivotal calcium metabolism regulator: calmodulin involved in shell formation from pearl oyster (Pinctada fucata). Comparative Biochemistry and Physiology Part A: Molecular & Integrative Physiology 138:235_243 DOI 10.1016/j.cbpc.2004.03.012.

Li S, Huang J, Liu C, Liu Y, Zheng G, Xie L, Zhang R. 2016. Interactive effects of seawater acidification and elevated temperature on the transcriptome and biomineralization in the pearl oyster Pinctada fucata. Environmental Science & Technology 50:1157_1165 DOI 10.1021/acs.est.5b05107.

McLoughlin K, Turteltaub K, Bankaitis-Davis D, Gerren R, Siconolfi L, Storm K, Cheronis J, Trollinger D, Macejak D, Tryon V, Bevilacqua M. 2006. Limited dynamic range of immune response gene expression observed in healthy blood donors using RT-PCR. *Molecular Medicine* 12: 185-195.

Mitta G, Vandenbulcke F, Hubert F, Salzet M, Roch P. 2000. Involvement of mytilins in mussel antimicrobial defense. Journal of Biological Chemistry 275:12954_1262 DOI 10.1074/jbc.275.17.12954.

Parisi MG, Toubiana M, Mangano V, Parrinello N, Cammarata M, Roch P. 2012. MIF from mussel: coding sequence, phylogeny, polymorphism, 3D model and regulation of expression. Developmental & Comparative Immunology 36:688_696 DOI 10.1016/j.dci.2011.10.014.

Philipp EER, Kraemer L, Melzner F, Poustka AJ, Thieme S, Findeisen U, Schreiber S, Rosenstiel P. 2012. Massively parallel RNA sequencing identifies a complex immune gene repertoire in the lophotrochozoan Mytilus edulis. PLOS ONE 7:e33091 DOI 10.1371/journal.pone.0033091.

Poynton HC, Vulpe CD. 2009. Ecotoxicogenomics: emerging technologies for emerging contaminants. *Journal of the American Water Resources Association* 45: 83-96.

Romero A, Estévez-Calvar N, Dios S, Figueras A, Novoa B. 2011. New insights into the apoptotic process in mollusks: characterization of caspase genes in Mytilus galloprovincialis. PLOS ONE 6:e17003 DOI 10.1371/journal.pone.0017003.

Tsan MF, Gao B. 2004. Cytokine function of heat shock proteins. American Journal of Physiology-Cell Physiology 286:C739_C744 DOI 10.1152/ajpcell.00364.2003.

Wu R. 2002. Hypoxia: from molecular responses to ecosystem responses. Marine Pollution Bulletin 45:35_45 DOI 10.1016/S0025-326X(02)00061-9.

APPENDIX

Table 3. Medians and ranges calculated for mussels (adductor muscle tissue) sampled at LTEMP sites in 2019 and 2020, as well as from PWS sites from 2012-2015.

	AMT19		AMT20		GB20		CoC19		GoC20		JB20	
	Median	**Range**	**Median**	**Range**	**Median**	**Range**	**Median**	**Range**	**Median**	**Range**	**Median**	**Range**
CaM	19.58	4.41	19.05	3.96	19.58	4.41	19.05	3.96	20.82	3.57	19.87	2.91
Casp8	14.11	3.41	14.54	4.29	14.11	3.41	14.54	4.29	15.63	4.77	13.33	2.28
MIF	19.59	8.99	20.23	3.91	19.59	8.99	20.23	3.91	18.56	11.01	20.60	7.99
Calponin	19.94	3.62	20.07	4.86	19.94	3.62	20.07	4.86	19.28	4.14	20.44	4.55
Chitinase	19.15	3.02	19.06	3.55	19.15	3.02	19.06	3.55	20.58	4.12	20.10	2.79
CCOIV	21.32	7.37	20.27	3.18	21.32	7.37	20.27	3.18	22.59	5.28	21.68	6.91
HSP70	14.06	5.98	11.55	2.99	14.06	5.98	11.55	2.99	13.75	4.66	13.44	4.21
HSP90	13.73	5.12	14.01	5.55	13.73	5.12	14.01	5.55	15.02	6.17	14.17	5.70
HIFa	15.65	2.30	14.64	3.78	15.65	2.30	14.64	3.78	16.14	4.27	16.37	3.46
MyticinB	16.34	6.49	14.88	12.20	16.34	6.49	14.88	12.20	16.45	12.29	13.93	11.16
Mytilin	18.73	3.70	17.52	6.91	18.73	3.70	17.52	6.91	17.96	8.15	16.86	7.03
MT20	9.85	2.83	8.87	2.58	9.85	2.83	8.87	2.58	10.19	5.25	9.45	3.93
Cyp3	17.30	3.49	16.13	3.69	17.30	3.49	16.13	3.69	17.11	4.76	15.98	4.32
P53	16.34	3.10	15.77	4.15	16.34	3.10	15.77	4.15	17.53	3.29	16.21	2.54

	JPO19		JPO20		VH19		VH20		PWS	
	Median	**Range**	**Median**	**Range**	**Median**	**Range**	**Median**	**Range**	**Median**	**Range**
CaM	21.24	11.09	20.32	6.43	16.82	5.04	19.92	5.56	19.96	9.60
Casp8	15.34	9.95	14.12	3.47	12.14	5.27	13.92	5.96	16.66	10.08
MIF	17.77	17.62	20.01	7.40	14.52	10.31	17.57	7.51	18.71	13.60
Calponin	21.35	10.38	18.36	5.05	18.40	5.33	18.89	5.57	21.58	32.39
Chitinase	21.24	7.94	19.65	3.65	18.11	1.80	20.48	5.32	20.27	23.04
CCOIV	21.99	9.97	21.20	6.94	17.83	11.78	21.06	8.14	22.11	14.28
HSP70	12.59	9.04	13.08	3.94	9.79	3.57	12.99	6.23	12.38	16.46
HSP90	13.12	9.49	14.96	4.18	13.28	4.58	14.29	6.16	14.36	11.64
HIFa	14.07	8.18	16.37	3.28	13.48	1.48	15.87	4.51	15.67	7.50
MyticinB	17.75	12.29	16.20	10.92	9.15	8.56	15.10	9.65	14.76	17.04
Mytilin	19.78	10.96	17.94	12.93	14.67	8.14	17.87	5.39	18.71	13.30
MT20	9.95	12.36	9.90	1.97	6.84	6.03	10.59	3.96	14.84	11.07
Cyp3	17.27	13.13	15.71	3.03	13.42	4.76	16.40	5.51	17.74	9.64
P53	15.83	10.17	16.58	3.15	13.15	4.28	16.07	5.30	18.61	28.03

Table 4. Medians and ranges calculated for mussels (gill tissues) sampled at LTEMP sites in 2019 and 2020, as well as from other studies in KATM and LACL (2015-2016) and PWS (2012-2015).

	AMT19		AMT20		GB20		GoC19		GoC20		JB20		JPO19	
	Median	**Range**	**Median**	**Range**	**Median**	**Range**	**Median**	**Range**	**Median**	**Range**	**Median**	**Range**	**Median**	**Range**
CaM	17.11	5.11	16.76	4.76	17.08	2.63	14.61	1.91	16.57	2.74	16.63	2.35	17.05	3.10
Casp8	9.47	3.54	8.80	2.65	9.74	3.28	8.62	2.55	9.73	4.94	9.46	1.82	9.59	3.34
MIF	17.36	9.52	17.00	8.00	18.75	8.49	17.75	2.88	16.48	9.81	18.75	7.89	16.33	14.68
Calponin	25.87	3.65	23.54	2.36	24.23	2.50	23.15	4.43	23.81	3.76	24.64	2.86	26.22	4.75
Chitinase	20.90	5.08	20.04	5.89	19.82	4.54	19.57	5.41	21.15	5.37	20.15	3.97	21.42	3.39
CCOIV	21.00	6.92	17.04	8.98	18.79	5.21	16.71	5.50	19.48	5.26	19.05	7.63	18.51	4.48
HSP70	11.87	6.04	12.21	5.94	13.03	9.98	10.25	1.78	11.90	4.03	13.02	4.53	11.93	6.07
HSP90	13.39	4.34	12.72	5.19	12.51	4.19	13.80	5.88	13.34	4.17	12.82	5.33	12.10	6.86
HIFa	13.52	2.50	14.24	3.12	13.20	3.97	13.01	2.76	13.90	4.24	13.74	4.61	12.73	3.78
MyticinB	9.01	13.36	13.10	10.26	12.79	8.03	10.93	9.51	12.64	13.73	12.75	11.24	15.05	12.36
Mytilin	15.79	4.26	14.26	2.99	14.88	3.79	14.35	5.01	14.03	8.98	15.13	6.67	16.10	4.44
MT20	6.51	4.35	7.11	5.02	6.57	3.11	5.24	1.62	6.91	5.72	6.80	2.08	5.99	7.19
Cyp3	12.53	3.67	13.58	3.98	14.15	3.57	12.98	4.22	15.33	5.11	13.60	3.72	13.31	4.17
P53	11.00	2.23	10.97	1.98	11.96	2.03	10.37	2.09	11.31	2.54	11.80	2.14	10.81	6.20

	JPO20		VH19		VH20		PWS		KATM		LACL	
	Median	**Range**	**Median**	**Range**	**Median**	**Range**	**Median**	**Range**	**Median**	**Range**	**Median**	**Range**
CaM	17.26	7.33	14.79	3.09	16.77	6.29	17.06	6.02	16.85	7.89	15.77	8.72
Casp8	9.63	4.08	9.51	4.30	9.46	4.65	11.79	5.89	10.60	5.56	10.27	9.89
MIF	18.09	6.48	14.22	8.17	15.87	12.12	19.49	8.93	18.06	10.31	17.84	11.30
Calponin	24.35	3.66	23.44	3.43	24.20	4.29	25.59	6.49	25.21	6.76	24.56	10.29
Chitinase	20.67	3.64	19.51	7.96	20.44	4.88	19.17	3.62	18.55	11.94	18.69	7.97
CCOIV	18.53	5.76	17.01	8.00	18.47	6.27	18.94	11.89	18.31	11.59	18.42	11.22
HSP70	12.51	5.32	10.47	4.21	12.21	4.79	11.92	5.70	12.13	8.59	11.03	11.37
HSP90	14.52	4.08	13.55	6.83	13.89	5.96	14.19	5.18	13.97	8.58	13.20	6.22
HIFa	13.80	3.90	12.84	6.17	14.28	3.11	14.83	3.42	14.33	3.87	13.89	5.78
MyticinB	12.89	10.03	7.14	8.64	12.50	13.58	11.79	13.42	13.73	13.74	11.56	15.05
Mytilin	15.04	10.83	13.86	6.37	14.66	6.22	15.94	8.62	16.40	10.25	15.54	8.76
MT20	6.93	4.19	5.44	3.02	7.61	6.35	12.77	10.20	10.60	13.46	8.83	14.51
Cyp3	13.66	4.39	13.39	2.97	14.16	5.94	15.79	7.10	14.96	5.61	13.95	11.44
P53	11.45	3.03	11.44	2.09	11.96	3.91	13.83	5.53	13.01	9.51	12.68	12.53